

## Article

# Searching for Sustainable-Irrigation Issues of Clementine Orchards in the Syrian Akkar Plain: Effects of Irrigation Method and Canopy Size on Crop Coefficients, Transpiration, and Water Use with SIMDualKc Model

Hanaa Darouich <sup>1,\*</sup>, Razan Karfoul <sup>2</sup>, Tiago B. Ramos <sup>3</sup> , Ali Moustafa <sup>2</sup> and Luis S. Pereira <sup>1</sup> 

<sup>1</sup> LEAF—Linking Landscape, Environment, Agriculture and Food Research Center, Associated Laboratory TERRA, Instituto Superior de Agronomia, Universidade de Lisboa, Tapada da Ajuda, 1349-017 Lisboa, Portugal; luis.santospereira@gmail.com

<sup>2</sup> General Commission for Scientific Agriculture Research (GCSAR), Hejaz Station, Damascus P.O. Box 113, Syria; rzoneh77@gmail.com (R.K.); moustali88@gmail.com (A.M.)

<sup>3</sup> Centro de Ciência e Tecnologia do Ambiente e do Mar (MARETEC-LARSyS), Instituto Superior Técnico, Universidade de Lisboa, Av. Rovisco Pais, 1, 1049-001 Lisboa, Portugal; tiagobramos@tecnico.ulisboa.pt

\* Correspondence: hdarouich@isa.ulisboa.pt

**Abstract:** Citrus is one of the most valuable crops in Syria, with the largest production areas in the Tartus and Latakia provinces. Water-saving policies have been adopted to modernize the irrigation systems and increase water productivity. Following dedicated research, this study aimed to evaluate the water balance in clementine trees irrigated with diverse methods and schedules using the SIMDualKc software model. Two experiments are reported: one with 10–14 years old trees irrigated with different methods (2007–2011) and the other with the same trees but now 18–20 years old, irrigated with different schedules (2015–2019). The SIMDualKc model successfully simulated the soil water contents measured in the various field plots, with root mean square error values lower than  $0.004 \text{ m}^3 \text{ m}^{-3}$  and modeling efficiencies up to 0.83. The model-calibrated standard basal crop coefficients ( $K_{cb}$ ) were approximately constant throughout all growing stages, assuming values of 0.54–0.55 for the mature trees having smaller height ( $h$ ) and fraction of ground cover ( $f_c$ ), and 0.64 for older trees with larger canopies, i.e., larger  $h$  and  $f_c$ . With drip irrigation, single  $K_c$  had a higher value (1.14) at the end, non-growing, and initial stages, and a lower value (0.75–0.76) during mid-season ( $K_{c \text{ mid}}$ ), because precipitation was lesser then, contributing less to soil evaporation. On the other hand,  $K_c$  values were nearly constant with micro-sprinkler and surface irrigation techniques because the ground was fully wetted. The  $K_{cb}$  values derived from the fraction of ground cover and height (A&P approach) were similar to those obtained from the model, thus showing that the A&P approach represents a practical alternative to estimate  $K_{cb}$  in the practice of irrigation management. The soil water balance further revealed a large weight of the terms corresponding to the non-beneficial water consumption and non-consumptive water use when the fraction wetted was large and the application efficiencies were low. These terms were reduced, namely, evaporation losses when drip irrigation was used. This study, thus, provides a valuable tool for improving the irrigation management, water saving, and water productivity of Syrian citrus production systems.

**Keywords:** FAO dual  $K_c$  approach; irrigation methods; irrigation scheduling; non-beneficial water consumption; non-consumptive water use



**Citation:** Darouich, H.; Karfoul, R.; Ramos, T.B.; Moustafa, A.; Pereira, L.S. Searching for Sustainable-Irrigation Issues of Clementine Orchards in the Syrian Akkar Plain: Effects of Irrigation Method and Canopy Size on Crop Coefficients, Transpiration, and Water Use with SIMDualKc Model. *Water* **2022**, *14*, 2052. <https://doi.org/10.3390/w14132052>

Academic Editor: Xinchun Cao

Received: 27 May 2022

Accepted: 21 June 2022

Published: 27 June 2022

**Publisher's Note:** MDPI stays neutral with regard to jurisdictional claims in published maps and institutional affiliations.



**Copyright:** © 2022 by the authors. Licensee MDPI, Basel, Switzerland. This article is an open access article distributed under the terms and conditions of the Creative Commons Attribution (CC BY) license (<https://creativecommons.org/licenses/by/4.0/>).

## 1. Introduction

Citrus is a major commercial produce in the Mediterranean region, even though its origins are in Southeast Asia [1]. The citron (*Citrus medica* L.) was the first species introduced in the region via Persia in the 5–4th centuries BC. The most important species, such as sweet orange (*Citrus sinensis* (L.) Osbeck) and mandarin (*Citrus reticulata* Blanco), reached the

Mediterranean basin later, in the 15th and 19th centuries AD, respectively [1,2]. Nowadays, the Mediterranean produces nearly 20% of the world's citrus and accounts for 60% of the world fresh citrus trade [3]. According to FAO statistics [4], Spain (3.45 M tons year<sup>-1</sup>), Egypt (3.08 M tons year<sup>-1</sup>), and Italy (1.65 M tons year<sup>-1</sup>) were the main producers of orange in the Mediterranean during the 2016–2020 seasons, with Syria ranking 6th, averaging 0.67 M tons year<sup>-1</sup>. For lemons and limes, Spain (0.99 M tons year<sup>-1</sup>), Italy (0.44 M tons year<sup>-1</sup>), and Syria (0.36 M tons year<sup>-1</sup>) topped the production ranking during that same period (2016–2020). Clementine (*Citrus clementina* Hort.) is also a popular citrus crop in Syria.

Citrus cultivation, including clementine, initiated in Syria in the 1970s, rapidly increasing after 1986 in response to government policies [5]. Today, the cultivated area is close to 42,700 ha, mainly in the Tartus and Latakia provinces, which combine favorable environmental conditions, namely, mild winters, high humidity for most of the year, annual rainfall averaging more than 800 mm, and water availability for irrigation during the dry summer season [5,6]. Citrus production counts as an important income source for the country, representing 1.3% of the gross domestic product, 20% of the value of national fruit and vegetable exports, and 0.8% of the world global production [5].

Although annual rainfall is higher in the Tartus and Latakia provinces than in other parts of Syria, agricultural production, citrus included, much depends on irrigation during the dry summer season. In those provinces, traditional surface methods are used in 55% of the irrigated land area, while modern methods such as dripping represent 43% of the irrigated surface [7]. This is a direct result of the water-saving policies implemented in Syria over the last decades, before war time. Such policies aimed at rationalizing agricultural water use and avoiding the overexploitation of available water resources [8–12], improving land and water productivity and farmers' income [13]; assessing and comparing the performance of surface, drip, and sprinkler irrigation systems [14–16]; and protecting groundwater and surface water resources from diffuse pollution [17]. Yet, despite great advances, water security issues and associated environmental risks still remain due to the poor irrigation water management and over-fertilization of crops [6,18–20]. This study was conducted in the Akkar region, located in the coastal area between Tripoli, in Lebanon, and Tartus, in Syria. The region is adversely characterized by poor drainage conditions, occurrence of flooding, and the lack of dependable water supply and distribution systems, which further emphasizes the need for better management of soil and water resources [21].

The efficient use of water resources in citrus production systems has become a top priority of research in Syria and other countries, with studies focusing on the accurate estimate of citrus water requirements [22–27], irrigation scheduling and crop response to water stress [28–30], and crop response to irrigation methods and systems layout [31,32], as well as agricultural water productivity [33,34]. There is still little information on the effect of canopy cover, plant height, tree age, and irrigation methods on the crop coefficient and citrus water requirements to more adequately provide accurate irrigation scheduling information to farmers.

Most of the studies referred to above used the FAO56 method for computing crop water requirements or for reference comparison among field measurements following approaches documented by Allen et al. [35,36]. The FAO56 method is widely used for estimating crop evapotranspiration ( $ET_c$ ) as the product of a crop coefficient ( $K_c$ ) and the grass reference evapotranspiration ( $ET_o$ ), the latter being calculated with the FAO Penman–Monteith (FAO-PM) equation [37].  $K_c$  values are defined for each crop stage by following the single crop coefficient approach, which assumes a single value for considering both the soil evaporation and crop transpiration processes, or the dual crop coefficient approach ( $K_c = K_{cb} + K_e$ ), which separately considers the basal transpiration coefficient ( $K_{cb}$ ) and the soil evaporation coefficient ( $K_e$ ). Rallo et al. [38] provided a review on single and dual  $K_c$  for different citrus species in various parts of the world, as well as for other fruit trees and vines, which served as reference for the current study. While the single  $K_c$  approach is simpler to use, the dual  $K_c$  approach is more precise for estimating evapotranspiration,

particularly as it allows both the soil evaporation and the transpiration components to be estimated [39,40].

The dual  $K_c$  approach has been applied worldwide for a variety of crops, climate soils, and management practices [41–44]; however, it has rarely been applied for citrus. This  $K_c$  approach is adopted in the SIMDualKc model [45] for computing evapotranspiration fluxes and partitioning ET into crop transpiration and soil evaporation; it has also been successfully applied for a range of crops and environmental and management conditions [46–50]. In Syria, SIMDualKc applications include rain-fed and surface-irrigated wheat in Aleppo [51], and zucchini squash and jute mallow under diverse irrigation regimes in the study area, the Akkar plain [52,53].

The objectives of this study are, thus, (i) to calibrate and validate the SIMDualKc software model for both sets of data, with smaller and larger canopies; (ii) to derive the  $K_c$  and  $K_{cb}$  standard crop coefficients for clementine trees grown in the Akkar region using SIMDualKc; (iii) to compare the hydric behavior of the former and more recent data sets to assess the effects of training on smaller or larger canopies; and (iv) to assess the impacts of irrigation methods on  $K_c$  and the terms of soil water balance and use. Two experimental data sets were used: one, from 2007 to 2011, where the water use of 10–14 years old citrus trees irrigated with different methods (surface, drip, mini-sprinklers, and bubblers) is compared; the other, from 2015 to 2019, where the water use of the same citrus trees, now 18–20 years old but drip-irrigated, are assessed. Following Darouich et al. [52,53], these assessments aim at improving water use in the Akkar plain and the sustainability of local production systems by providing a state-of-the-art tool for irrigation scheduling based on the FAO56 dual  $K_c$  method. Innovation consists of using a dual  $K_c$  soil water balance model to compute and compare diverse citrus orchard irrigation methods to accurately determine dual and single  $K_c$  for clementine as dependent on the canopy cover, tree height, irrigation method, and scheduling, which still are lacking in practice. The ultimate objective is the development and implementation of water-saving irrigation practices, the assessment of which shall be the object of a companion paper to be published later.

## 2. Materials and Methods

### 2.1. Field Experiment

#### 2.1.1. Description of the Study Site

This study was carried out at the Zahid research station, in the western part of the Akkar plain, Tartus governorate, Syria (34°41'37" N, 35°59'16" E; 12 m a.s.l.). The first part of this research study (hereafter referred to as Experiment 1 or E1) was performed from 2007 to 2011, while the second part (Experiment 2 or E2) was developed from 2015 to 2017 (Table 1).

**Table 1.** Experiments reported in this study.

Experiment	Years	Tree Age	Plot	Irrigation Method
E1	2007–2011	10–14	E1.1	Drip
			E1.2	Bubblers
			E1.3	Micro-sprinklers
			E1.4	Ring basins
E2	2015–2017	18–20	E2.1	Drip, moderate deficit
			E2.2	Drip, mild deficit
			E2.3	Drip, full irrigation

Previous studies [52,53] performed in the same research station aimed at estimating the crop coefficients of zucchini squash (*Cucurbita pepo* L.) and jute mallow (*Corchorus olitorius* L.) under different irrigation regimes were developed in fields close to the one now used.

The climate in the region is hot-summer Mediterranean (Csa) [54]. The surface air temperature averages 19.3 °C over the year, with mean daily values varying from 11.5 °C in January to 27.0 °C in August. The annual precipitation averages 930 mm and occurs

mostly between October and May. The daily reference evapotranspiration ( $ET_0$ ) was computed with the FAO56 PM equation [37], and its annual average was 1363 mm for the period of 1998–2020. The daily weather data used in this study were taken from the local meteorological station installed over well-watered clipped grass and are given in Figure 1. The collected data included the daily values of maximum and minimum air temperatures ( $T_{max}$  and  $T_{min}$ ; °C), sunshine hours ( $H_{sun}$ ; h), maximum and minimum relative humidity ( $RH_{max}$  and  $RH_{min}$ ; %), wind speed measured at a 2 m height ( $u_2$ ;  $m\ s^{-1}$ ), and rainfall ( $P$ ; mm). It may be seen that there was not a great interannual variability of the climate variables except for precipitation and, less, for  $ET_0$ .

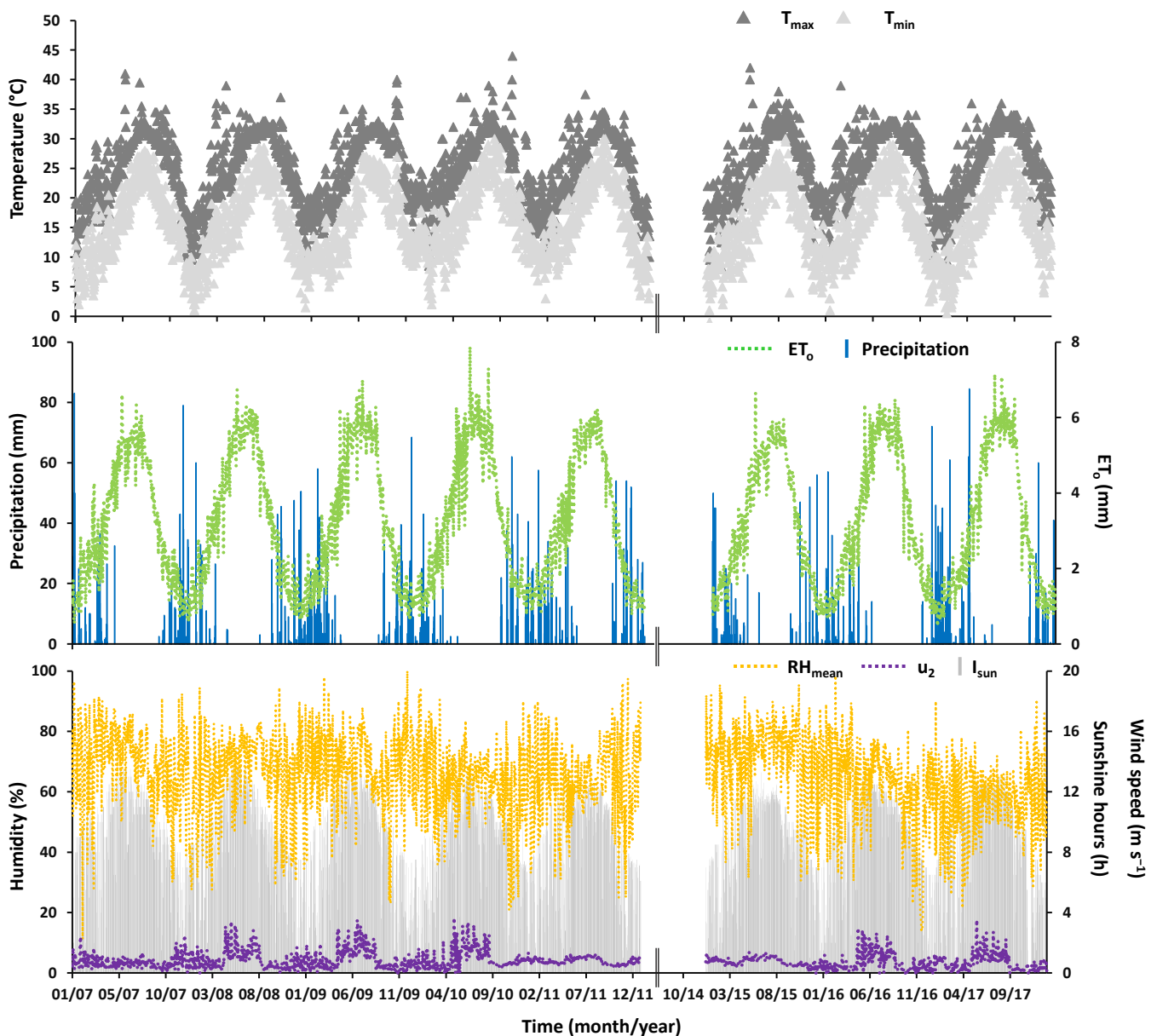


**Figure 1.** Daily maximum ( $T_{max}$ ; °C) and minimum ( $T_{min}$ ; °C) air temperatures, mean relative humidity ( $RH_{mean}$ ; %), number of sunshine hours ( $I_{sun}$ ; h), wind speed at a 2 m height ( $u_2$ ;  $m\ s^{-1}$ ), precipitation (mm), and grass reference evapotranspiration ( $ET_0$ ; mm) for the 2007–2011 and 2015–2017 years.

The dominant soil reference groups in the Akkar plain are Vertisols, Cambisols, and Luvisols [55]. Irrigated agricultural land, which is supplied by surface water resources, covers 29,100 ha in the Tartus district and 38,000 ha in the Latakia district [7]. Those

resources are complemented with groundwater resources, the water table depth of which varies from 10 to 20 m [19].

### 2.1.2. Experimental Design and Treatments

The clementine trees (cv. Common with rootstock *Citrus aurantium*) were transplanted to the field in 1998, when they were 1 year old, in an area 70 m long and 45 m wide (3150 m<sup>2</sup>) with slopes of 0.005% and 0.002% in the west and south directions, respectively. The soil was Vertisol [56], with the main physical and chemical properties given in Table 2. The sampling details and methodologies used in the determination of soil properties were identical to those reported in Darouich et al. [52,53] and can be found in those publications. A subsurface drainage network was buried at depths of 1.25–1.75 m, with drainpipes spacing 15–25 m, to collect excess water. The experimental field was surrounded by windbreak trees, distancing 4.5–6.0 m from the clementine trees.

**Table 2.** Main soil physical and chemical properties of the experimental area.

Depth (m)	Soil Texture (%)			$\rho_b$ (g cm <sup>-3</sup> )	OM (%)	Soil Water Contents			TAW (mm)
	Sand (2–0.05 mm)	Silt (0.05–0.002 mm)	Clay (<0.002 mm)			$\theta_s$ (m <sup>3</sup> m <sup>-3</sup> )	$\theta_{FC}$ (m <sup>3</sup> m <sup>-3</sup> )	$\theta_{WP}$ (m <sup>3</sup> m <sup>-3</sup> )	
0.0–0.15	15	28	57	1.24	2.2	0.53	0.51	0.23	42
0.15–0.30	16	32	52	1.25	2.0	0.53	0.47	0.24	35
0.30–0.45	20	30	50	1.30	1.9	0.51	0.48	0.24	35
0.45–0.60	19	28	53	1.43	-	0.53	0.51	0.30	32
0.60–0.75	22	28	50	1.26	-	0.52	0.42	0.24	27
0.75–0.90	22	28	50	1.26	-	0.55	0.45	0.24	31
0.90–1.05	20	28	52	1.26	-	0.55	0.45	0.25	30

Note:  $\rho_b$ , bulk density; OM, organic matter content;  $\theta_s$ , soil water content at saturation;  $\theta_{FC}$ , soil water content at field capacity;  $\theta_{WP}$ , soil water content at the wilting point; TAW, total available water.

Tree spacing was 5 m × 5 m; thus, crop density was 400 trees ha<sup>-1</sup>. The trees were trained in the typical vase system, with pruning performed every 4 years just before the crop development phase, i.e., from early to mid-February. In E1, trees were pruned in 2007 and 2011. In E2, pruning was in 2015. Table 3 presents the dates of the crop development stages and the respective cumulative growing-degree days (GDDs) for the studied seasons. The GDDs were computed from the difference between the daily mean temperature and a base temperature ( $T_{base}$ ) of 12.8 °C, in agreement with the range of values (12–13 °C) reported in the literature [57–59]. The dates of the crop stages were not far from those reported in the literature for diverse areas in the Mediterranean region [34,60,61].

**Table 3.** Dates of the crop growth stages and growing-degree days (GDDs) during the experimental seasons.

Year	Crop Growth Stages						Non-Growing	Total GDDs
	Non-Growing	Initial	Crop Development	Mid-Season	Late-Season	End-of-Season		
Experiment 1								
2007	1 January	3 February	18 February	8 June	1 October	8 December	31 December	-
GDDs	-	40	574	1561	554	-	-	2728
2008	1 January	10 February	10 March	1 June	22 September	9 December	31 December	-
GDDs	-	56	565	1568	655	-	-	2844
2009	1 January	26 January	26 February	9 June	1 October	4 December	31 December	-
GDDs	-	35	508	1559	546	-	-	2648
2010	1 January	1 February	1 March	26 May	21 September	12 December	31 December	-
GDDs	-	58	542	1681	689	-	-	2971
2011	1 January	13 February	4 March	25 May	24 September	19 November	31 December	-
GDDs	-	71	527	1685	460	-	-	2743
Experiment 2								
2015	1 January	6 February	8 March	5 June	1 October	9 December	31 December	-
GDDs	-	35	503	1648	527	-	-	2714
2016	1 January	31 January	16 February	24 May	5 October	30 November	31 December	-
GDDs	-	29	638	1857	449	-	-	2973
2017	1 January	3 February	3 March	1 June	25 September	5 December	31 December	-
GDDs	-	14	540	1688	578	-	-	2820

Experiment 1 (E1) involved the irrigation of the clementine orchard using different irrigation methods (drip, bubblers, mini-sprinklers, and surface) during five growing seasons (2007–2011) (Table 1). Trees were 10–14 years old, and tree height ranged from 2.5 to 3.0 m. The experimental area was divided into four treatments (E1.1, E1.2, E1.3, E1.4) according to the scheme indicated in Figure 2. E1.1 covered 800 m<sup>2</sup>, with 32 clementine trees. Trees were drip-irrigated, with 4 drippers per tree and discharge rates of 8 L h<sup>-1</sup> under an operative pressure of 1.0–1.5 bar. E1.2 covered 825 m<sup>2</sup>, with 33 clementine trees. Trees were irrigated by bubblers (1 per tree), at a discharge rate of 60 L h<sup>-1</sup> under an operative pressure of 2.0–2.5 bar. E1.3 covered 800 m<sup>2</sup>, with 32 clementine trees. Trees were irrigated by mini-sprinklers (1 per tree) at a discharge rate of 60 L h<sup>-1</sup> under an operative pressure of 2.0–2.5 bar. E1.4 covered 550 m<sup>2</sup>, with 22 clementine trees. Trees were surface-irrigated using ring basins with a radius of 1.5–2.0 m, about equal to the radius of the trees' canopies. The water was supplied upstream at a discharge rate of 1.4 m<sup>3</sup> h<sup>-1</sup> and the ring basins were connected along the tree rows.

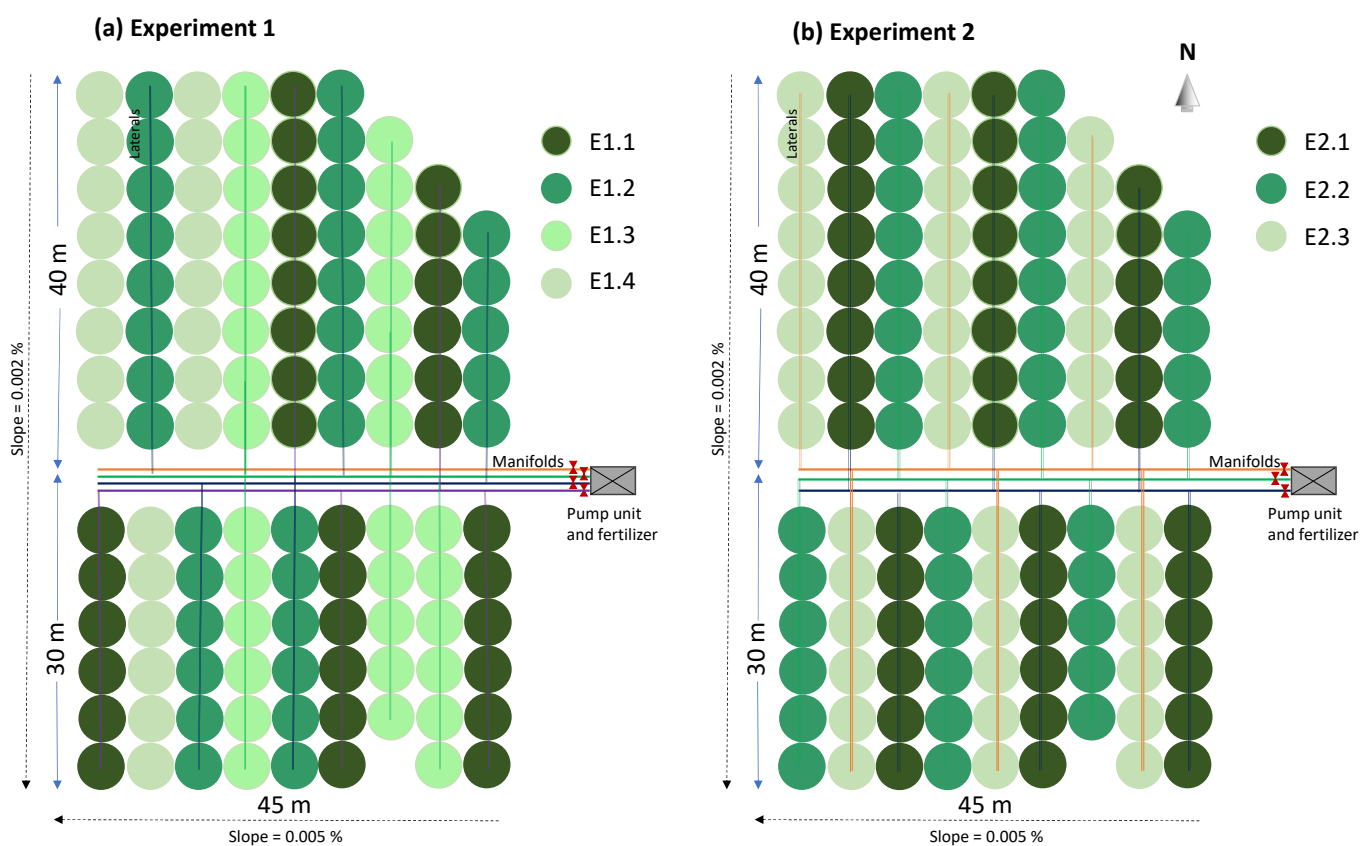


**Figure 2.** Experimental schemes in experiments (a) E1 (2007–2011) and (b) E2 (2015–2017).

The water was transported from a well to the field by a PVC mainline and distributed to four polyethylene manifold pipes. One lateral supplied each tree row in the plots with pressurized irrigation systems (i.e., drip, bubblers, and mini-sprinklers). Each E1 treatment registered the same net irrigation amount and frequency (Table 4). Irrigation was triggered when soil water contents in the rootzone dropped below 90% of  $\theta_{FC}$ . Net irrigation amounts were determined based on the measurements of field irrigation efficiency for the studied irrigation method following the guidelines in Merriam and Keller [62], with dripping, bubblers, mini-sprinklers, and ring basins assuming values of 90%, 86%, 84%, and 68%, respectively. Irrigation was performed from mid-April to the end of October and thus out of the rainfall season.

**Table 4.** Irrigation depths and events during the E1 seasons.

Year	Number of Events	Depth (mm)	Total (mm)
2007	16	49	780
2008	16	49	780
2009	16	50	792
2010	16	51	816
2011	15	52	784

Experiment 2 (E2) concerned the drip irrigation of the clementine orchard according to various irrigation schedules during three growing seasons (2015–2017) (Table 1). Trees were 18–20 years old, and tree height ranged from 3.8 to 4.0 m. The experimental area was divided into three treatments (E2.1, E2.2, E2.3) as described in the scheme presented in Figure 2. E2.1 covered 1000 m<sup>2</sup>, with 40 clementine trees; E2.2 covered 950 m<sup>2</sup>, with 38 trees; and E2.3 covered 1025 m<sup>2</sup>, with 41 trees. Double laterals supplied each tree row, with 8 in-line drippers per tree and discharge rates of 8 L h<sup>-1</sup> under an operative pressure of 1.0–1.5 bar. All treatments aimed to fulfill crop water requirements but while applying different irrigation depths and schedules (Table 5). In E2.1, irrigation depths varied from 15 to 30 mm per event and were applied with an average frequency of 7 days. In E2.2, depths ranged from 33 to 44 mm per event, with an average frequency of 10 days. In E2.3, depths varied from 41 to 54 mm per event, with water applied every 15 days. Irrigation was also performed from mid-April to the end of October.

**Table 5.** Irrigation depths and events during the E2 seasons.

Year	E2.1			E2.2			E2.3		
	Number of Events	Depth (mm)	Total (mm)	Number of Events	Depth (mm)	Total (mm)	Number of Events	Depth (mm)	Total (mm)
2015	20	15–21	368	17	33–34	535	13	41–43	502
2016	21	17–30	490	18	34–37	608	14	33–49	588
2017	20	21–30	493	16	29–44	620	13	30–54	590

In both E1 and E2, irrigation depths and the dates of irrigation events were estimated following a simple water budget procedure in the field based on the atmospheric demand assumed equal to ET<sub>0</sub> and soil moisture data. The latter were measured with a neutron probe at depths of 0.3 and 0.6 m, at three locations per treatment every 7–10 days. In each treatment, the first insert tube was placed next to a clementine tree; the second, in the tree row between two trees (i.e., 2.5 m from the nearby trees) and at 1.0–1.5 m from the closest dripper; and the third, in the middle of the inter-row (also 2.5 m from the nearby trees) and at about 2 m from the drip lines. Measurements were then averaged for each location, and the measured values at 0.6 m were extended to the corresponding root depth of 1.0 m.

Additional management practices included fertilization with phosphorus (0.25 kg P<sub>2</sub>O<sub>5</sub> tree<sup>-1</sup>) and potassium (0.5 kg K<sub>2</sub>O tree<sup>-1</sup>) in autumn. Nitrogen was applied (1.0 kg N tree<sup>-1</sup>) in two batches, half at the beginning of the growing season (from late January to the beginning of February) and the rest with irrigation throughout the rest of the growing periods. Weeds were controlled in the rows and inter-rows with Glyphosate application in spring and manually whenever necessary. Harvest was usually from November to the end of the year. The tree orchard was hit by *Phytophthora citrophthora* between 2003 and 2007, affecting crop production in those years. The treatment involved the removal of the affected branches and the application of a copper-based fungicide to reduce the rate of infection.

## 2.2. Modelling Approach

### 2.2.1. The SIMDualKc Model

The SIMDualKc model [45,51] simulates the daily soil water balance and computes the actual crop ET at the crop-field scale adopting the FAO56 dual K<sub>c</sub> method [37,63]. The daily soil water equation is:

$$D_{r,i} = D_{r,i-1} - (P - RO)_i - I_i - CR_i + DP_i + ET_{c,act,i} \quad (1)$$

where  $D_r$  is the root-zone depletion (mm);  $P$  is the rainfall (mm);  $RO$  is the runoff (mm);  $I$  is the net irrigation depth (mm);  $CR$  is the capillary rise from the groundwater table (mm);  $DP$  is the deep percolation (mm); and  $ET_{c,act}$  is the actual crop evapotranspiration (mm), which is the main output of the soil water balance. All variables refer to the end of day  $i$ , or, in case of  $D_r$ , the day before,  $i-1$ .  $ET_{c,act}$  is computed as the product between the reference  $ET_o$  (mm d<sup>-1</sup>) and a crop coefficient ( $K_c$ ; dimensionless). In the current application, a dual  $K_c$  was used ( $K_c = K_{cb} + K_e$ ), where  $K_{cb}$  represents the ratio of actual transpiration ( $T_{c,act}$ ) to  $ET_o$  and  $K_e$  is the ratio between soil evaporation ( $E_s$ ) and  $ET_o$ .  $DP$  was calculated with the parametric equations described by Liu et al. [64], and  $RO$  was estimated using the curve number (CN) approach [65].  $CR$  was not considered in this study because the water table was at a depth greater than 10 m.

The flux diagram of the model (Figure 3) identifies the data required, the main calculation algorithms, and the diverse type of model outputs. Further details of the SIMDualKc model are provided in Rosa et al. [45] and described in various papers, in particular relatively to drip-irrigated olive orchards and vineyards [66,67]. The model makes possible several irrigation management options, as identified in the flowchart. The current application refers to the calibration and validation of the model for a clementine crop cultivated under well-defined environment, irrigation, and cropping conditions for the computation of the water balance terms using the dual  $K_c$  approach. After calibration and validation, the model can be used to develop and assess diverse irrigation scheduling options for application in the field.

The model computes crop evapotranspiration ( $ET_c$ ; mm) using the dual  $K_c$  approach, i.e., partitioning  $ET_c$  into transpiration ( $T_c$ ; mm) and soil evaporation ( $E_s$ ; mm). That partition is based upon the knowledge of the ground fraction shadowed by the crop ( $f_c$ ), which controls the amount of energy available for soil evaporation. It is then possible to separately determine the following [37,45,68]:

$$T_c = K_{cb} ET_o \quad (2)$$

$$E_s = K_e ET_o \quad (3)$$

where  $K_{cb}$  is the potential basal crop coefficient (-);  $K_e$  is the evaporation coefficient (-); and  $ET_o$  is the grass reference evapotranspiration (mm) defined with the FAO56 PM approach [37]. Actual  $T_c$  values ( $T_{c,act}$ ; mm) are reduced when water stress occurs, with values obtained using a multiplier stress coefficient ( $K_s$ ) with  $K_{cb}$ :

$$T_{c,act} = K_s K_{cb} ET_o = K_{cb,act} ET_o \quad (4)$$

where  $K_{cb,act}$  is the actual basal crop coefficient ( $K_{cb,act} < K_{cb}$ ) and  $K_s$  depends upon the depleted soil water on day  $i$  ( $D_{r,i}$ ; mm):

$$K_s = \frac{TAW - D_{r,i}}{TAW - RAW} \quad (5)$$

where  $TAW$  and  $RAW$  are the total and readily available soil water (mm), respectively, relative to the rooting depth. Assuming that the soil water depletion fraction for no stress is  $p$ , then  $RAW = p TAW$ . When depletion  $D_r$  exceeds fraction  $p$ , the available soil water drops

below the RAW resulting in  $K_s < 1.0$  (Equation (5)); then,  $T_{c\ act}$  reduces below potential  $T_c$ ; otherwise,  $K_s = 1.0$ , and no water stress occurs.

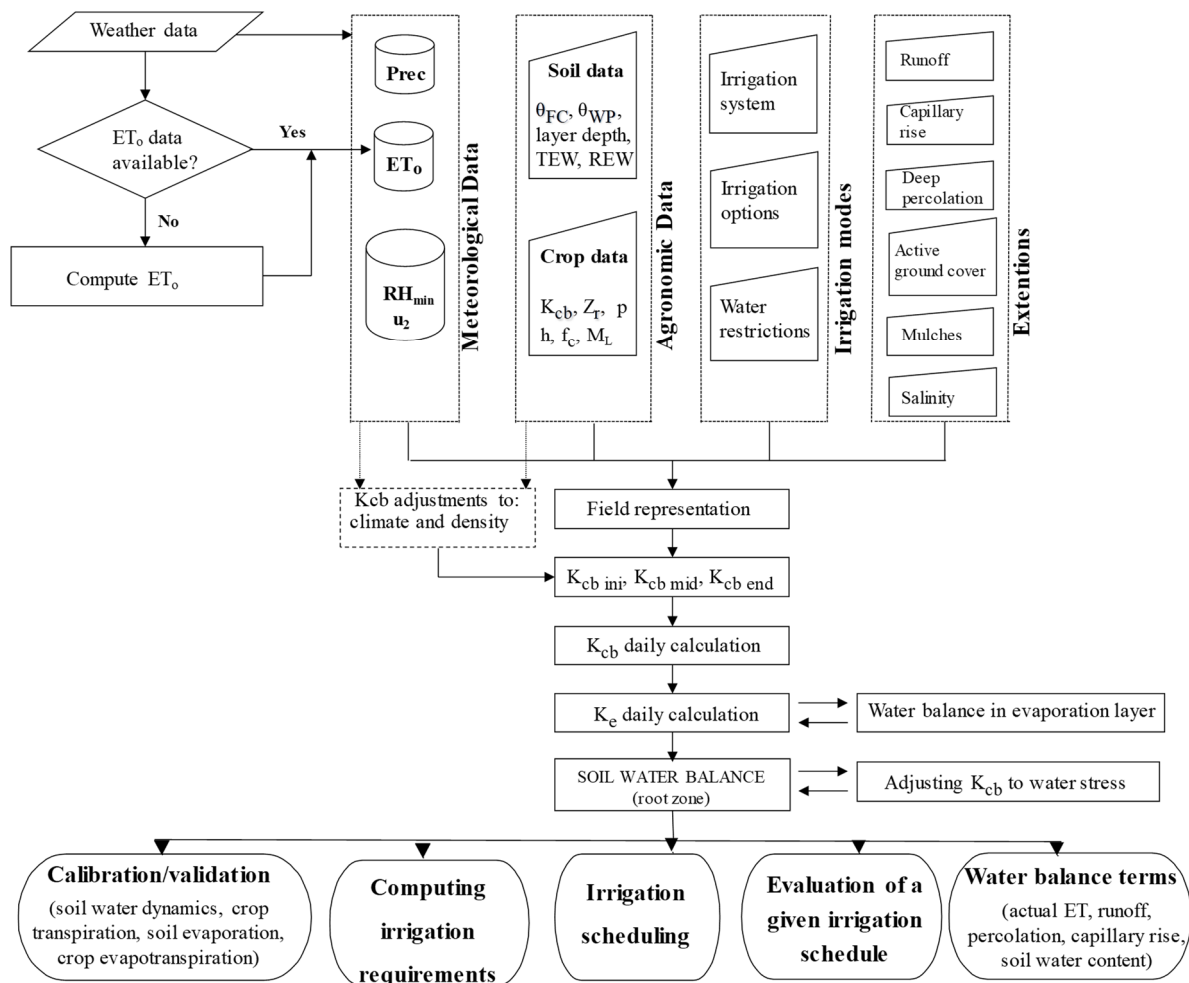


**Figure 3.** Schematic representation of SIMDualKc model (Adapted with permission from Rosa et al. [45]. Copyright 2012 Elsevier).

Soil evaporation is restricted by the amount of energy available on the soil surface, which adds to the energy consumed by transpiration, and by the water available in the surface soil layer with depth  $Z_e$  (m) [37,68].  $E_s$  is larger after pruning when the shadowed soil surface by the crop is decreased.  $E_s$  is smaller when the soil is not wetted and when there is ground cover by mulch and/or active ground cover. The evaporation coefficient ( $K_e$ ) is computed as:

$$K_e = K_r(K_{c\ max} - K_{cb\ min}) \leq f_{ew} K_{c\ max} \tag{6}$$

where  $K_r$  is the evaporation reduction coefficient (0–1);  $K_{c\ max}$  is the maximum value of  $K_c$  (i.e.,  $K_{cb} + K_e$ ) following rain or an irrigation event (–);  $K_{cb\ min}$  is the minimum value for  $K_{cb}$ ; and  $f_{ew}$  represents the fraction of soil wetted and directly exposed to solar radiation. It may be computed as:

$$f_{ew} = \min(1 - f_c, f_w) \tag{7}$$

i.e., the minimum value between the fraction of ground non-covered (non-shaded) by the vegetation canopy ( $1 - f_c$ ) and the fraction wetted by irrigation ( $f_w$ ).  $K_r$  is obtained using the two-stage drying cycle approach [37,68], where the first stage is energy limited and the

second is water limited. By comparing evaporation depletion  $D_{e,i-1}$  (mm) with the easily evaporable water REW (mm), it results:

$$K_r = 1 \quad \text{for } D_{e,i-1} \leq \text{REW} \quad (8)$$

$$K_r = \frac{\text{TEW} - D_{e,i-1}}{\text{TEW} - \text{REW}} \quad \text{for } D_{e,i-1} > \text{REW} \quad (9)$$

where TEW is the maximum depth of water that can be evaporated from a fully wetted evaporation soil layer (mm); REW is the depth of water that can be easily evaporated without water availability restrictions (mm); and  $D_{e,i-1}$  is the evaporation layer depletion at the end of day  $i - 1$  (mm).  $D_e$  is computed through a daily water balance of the evaporation soil layer with depth  $Z_e$  (m). The evaporation decreases as the evaporable soil water diminishes in the evaporation soil layer beyond the REW. Further information on the computational procedures adopted in SIMDualKc is provided by Rosa et al. [45] and Pereira et al. [40].

The  $K_{cb}$  values for the initial ( $K_{cb \text{ ini}}$ ), mid-season ( $K_{cb \text{ mid}}$ ), and end of season stages ( $K_{cb \text{ end}}$ ) are computed by the model when initial  $K_{cb}$  values are input to initiate the model calibration. Commonly, standard  $K_{cb \text{ mid}}$  and  $K_{cb \text{ end}}$  values are used for this purpose. Then, as proposed by Allen et al. [37], these standard values are internally corrected to become adjusted to local climatic conditions when the average minimum relative humidity ( $\text{RH}_{\text{min}}$ ) differs from 45% and/or when the average wind speed at a 2 m height ( $u_2$ ) differs from  $2 \text{ m s}^{-1}$ . Alternatively,  $K_{cb}$  values may be computed with the A&P approach as described below.

### 2.2.2. $K_{cb}$ from Fraction of Ground Cover and Height

The value for  $K_c$  decreases when the plant density or leaf area is below full ground cover in proportion to the amount of canopy vegetation. Thus, because  $K_{cb}$ , which mostly represents the transpiration component, is correlated with the amount of vegetation, it can be expressed in terms of a crop density coefficient,  $K_d$  [69,70]:

$$K_{cb} = K_{\text{min}} + K_d (K_{cb \text{ full}} - K_{c \text{ min}}) \quad (10)$$

where  $K_d$  is the density coefficient that represents the impacts of plant density and/or leaf area;  $K_{cb \text{ full}}$  is the estimated basal  $K_{cb}$  for plant growth conditions having nearly full ground cover (or  $\text{LAI} > 3$ ); and  $K_{c \text{ min}}$  is the minimum  $K_c$  for bare soil (in the absence of vegetation), the common value of which is about 0.15 under typical agricultural conditions. In orchards, natural vegetation or grass covering the ground for enhancing the infiltration of rainfall and/or reducing soil erosion is commonly found, which may compete with fruit trees for the available soil water, but which contributes to the total evapotranspiration of the orchard. In SIMDualKc, that contribution to  $\text{ET}_c$  is estimated as [65,69]:

$$K_{cb} = K_{cb \text{ cover}} + K_d \max \left[ (K_{cb \text{ full}} - K_{cb \text{ cover}}), \frac{K_{cb \text{ full}} - K_{cb \text{ cover}}}{2} \right] \quad (11)$$

where  $K_{cb \text{ cover}}$  is the  $K_{cb}$  of the ground cover in the absence of tree foliage;  $K_d$  is the density coefficient; and  $K_{cb \text{ full}}$  is the basal  $K_{cb}$  anticipated for the crop under full-cover conditions and corrected for climate. The second term of the max function, which accounts for the effects of the shading by the active ground cover, reduces the estimated  $K_{cb}$  by half the difference between  $K_{cb \text{ full}}$  and  $K_{cb \text{ cover}}$  when this difference is negative. The value for  $K_{cb \text{ cover}}$  in Equation (11) should represent the  $K_{cb}$  of the surface cover in the absence of tree cover; therefore, it should reflect the density and vigor of the surface cover as in areas exposed to sunlight. Equation (11) was used in this study when active vegetation cover was present in the rows and in the inter-rows.

Density coefficient  $K_d$  is estimated from observations of the fraction of the ground covered by vegetation ( $f_c$ ) and plant height ( $h$ ) and describes the increase in  $K_c$  with increases in the amount of vegetation. As reviewed by Pereira et al. [70,71],  $K_d$  is estimated as:

$$K_d = \min\left(1, M_L f_{c \text{ eff}}, f_{c \text{ eff}}^{\left(\frac{1}{1+h}\right)}\right) \quad (12)$$

where  $f_{c \text{ eff}}$  is the effective fraction of the ground covered or shaded by vegetation (0.01–1) near solar noon;  $M_L$  is a multiplier on  $f_{c \text{ eff}}$  describing the effect of canopy density on shading and maximum relative ET per fraction of shaded ground (1.0–2.0); and  $h$  is the mean vegetation height (m).

The  $K_{cb \text{ full}}$  value represents an upper limit on  $K_{cb \text{ mid}}$  for vegetation with adequate water supply having full ground cover (and a LAI > 3). It is estimated as:

$$K_{cb \text{ full}} = F_r \left( \min(1.0 + k_h h, 1.20) + [0.04(u_2 - 2) - 0.004(RH_{\min} - 45)] \left(\frac{h}{3}\right)^{0.3} \right) \quad (13)$$

where  $u_2$  is the mean daily wind speed at a 2 m height ( $\text{m s}^{-1}$ ) during the crop growth period;  $RH_{\min}$  (%) is the mean daily minimum relative humidity during the growth period; and  $h$  is the mean plant height (m) during mid-season. Before climatic adjustment, an upper limit for  $K_{cb \text{ full}}$  is 1.20 (Equation (13)). The effect of crop height is considered through the sum  $(1 + k_h h)$ , with  $k_h = 0.1$  for tree and vine crops [70]. Higher  $K_{cb \text{ full}}$  values are expected for taller crops and when the local climate is drier or windier than the standard climate conditions ( $RH_{\min} = 45\%$  and  $u_2 = 2 \text{ m s}^{-1}$ ). When the vegetation shows more stomatal adjustment upon transpiration, parameter  $F_r$  applies an empirical adjustment ( $F_r < 1.0$ ), otherwise  $F_r = 1.0$ . For trees and vines,  $F_r$  is closer to 1.0 when crops exhibit great vegetative vigor;  $F_r$  decreases with limited water supply and due to pruning and training when the crop is stressed, and stomatal control occurs. It can be defined as [70]:

$$F_r = \frac{\Delta + \gamma (1 + 0.34 u_2)}{\Delta + \gamma \left(1 + 0.34 u_2 \frac{r_1}{r_{\text{typ}}}\right)} \quad (14)$$

where  $r_1$  and  $r_{\text{typ}}$  are the estimated actual mean leaf resistance and the typical leaf resistance ( $\text{s m}^{-1}$ ), respectively, for the vegetation in question;  $\Delta$  is the slope of the saturation vapor pressure vs. air temperature curve ( $\text{kPa } ^\circ\text{C}^{-1}$ ); and  $\gamma$  is the psychrometric constant ( $\text{kPa } ^\circ\text{C}^{-1}$ ), both relative to the period when  $K_{cb \text{ full}}$  is computed. When standard  $K_{cb}$  values are considered, e.g., as initial values of  $K_{cb}$  for calibration purposes,  $F_r = 1.0$  is assumed. Differently, when searching for actual  $K_{cb}$  values,  $F_r < 1.0$  are estimated, namely, with the support of the tabulated values in Pereira et al. [70]. Examples of the application of the A&P approach to estimate  $K_{cb \text{ A\&P}}$  for several vegetable, field, and perennial crops are available in Pereira et al. [71]. The application of this approach does not require calibration/validation if using the tabulated parameters. Nevertheless, when field data are available, a validation may be performed by comparing the  $K_{cb \text{ A\&P}}$  and  $K_{cb}$  computed from field data, e.g., with the SIMDualKc model. The practical application of the dual  $K_c$  approach for supporting day-to-day field irrigation management is likely easier when adopting the A&P approach [69], as recently reviewed [70,71].

### 2.3. Model Setup

The SIMDualKc model requires comprehensive data on weather conditions, soil properties, crop phenology, ground conditions (mulch or active ground cover), irrigation events, and irrigation system performance for computing the soil water balance.

Soil data included the granulometry and soil hydraulic properties of the different soil layers as listed in Table 2. The TAW (mm) was then computed as the sum of the product of the difference between the soil water contents at field capacity ( $\theta_{FC}$ ;  $\text{m}^3 \text{ m}^{-3}$ ) and at the wilting point ( $\theta_{WP}$ ;  $\text{m}^3 \text{ m}^{-3}$ ) relative to the different soil layers of the root zone and

respective layer thickness down to a 1.0 m depth. The maximum and readily evaporable depths (TEW and REW; mm) and the depth of the evaporation soil layer ( $Z_e$ ; m) were estimated using the textural and water retention characteristics of the surface layer [37,68]. The deep percolation parameters ( $a_D$ ,  $b_D$ ) relative to the respective parametric equations proposed by Liu et al. [64] were defined according to the soil texture data and soil hydraulic properties. The runoff was estimated with the curve number (CN) method considering the texture of the surface soil layer, soil surface conditions, and land use [65]. Lastly, the initial soil water depletion values in both the root zone and the evaporation soil layer were defined based on field observations taken in E1 and E2 fields at the beginning of each growing season, corresponding to 0–8% of TAW and 0–8% of TEW.

Crop phenology data referred to the observed dates of the initial, development, mid-season, and late-season stages, and since citrus is an evergreen crop, they included the non-growing season (Table 3). The default  $K_{cb\ ini}$ ,  $K_{cb\ mid}$ , and  $K_{cb\ end}$  values were defined according to Rallo et al. [38] using the measurements of  $f_c$  as reference (Table 6). The soil water depletion fraction values for no stress ( $p_{ini}$ ,  $p_{mid}$ ,  $p_{end}$ ) were also set for the same crop stages based on Allen et al. [37]. Tree height (Table 6) and mean canopy width were monitored at the beginning of the initial, mid-season and end-of-season stages using a tape. The  $f_c$  values were then defined as in Table 6, not showing significant variations throughout the seasons, in line with the field measurements of the canopy width. Lastly, root depth ( $Z_r = 1.0$  m) was observed in trenches opened at the end of the experiment.

**Table 6.** Measured fraction of the ground cover ( $f_c$ ) and tree height (h) during the E1 and E2 seasons.

Parameter	E1					E2		
	2007	2008	2009	2010	2011	2015	2016	2017
Pruning	Yes	No	No	No	Yes	Yes	No	No
$f_c$ (-)	0.46	0.47	0.50	0.50	0.48	0.75	0.77	0.77
h (m)	2.5	2.8	2.8	3.0	2.8	3.8	4.0	4.0

The soil in the tree rows and in the inter-row was covered with grass during the rainfall season (i.e., from October to March). The density of this active ground cover was set to 20%, with a fraction of ground cover ( $f_c$  cover) of 0.2 and a maximum height ( $h_{cover}$ ) of 0.20 m based on observations. The evaporation reduction due to the mulch effect created by the grass cover was set to 10%, following Paço et al. [66].

Finally, irrigation depths and the respective dates of events were specified according to observations. The fractions of the soil surface wetted by irrigation ( $f_w$ ) were also defined according to the field measurements as 0.25, 0.45, 0.60, and 0.70 in the drip, bubbler, mini-sprinkler, and ring basin treatments.

#### 2.4. Calibration and Validation of the SIMDualKc Model

The SIMDualKc model was calibrated following the same “iterative trial-and-error” procedure documented in Pereira et al. [72] and widely used in applications of this model. Calibration procedures consisted in modifying model parameters one at a time within reasonable ranges of values until the deviations between simulations of soil water contents and respective measurements were minimized. Calibration was carried out separately for E1 and E2 using the E1.1 (2011) and E2.3 (2016) data sets, respectively. Calibration aimed to best account for the differences in the  $K_{cb}$  values in trees with different ages and heights while making sure that the parameters relative to soil properties were set the same in both experiments.

Model calibration started using E1 SWC data by first adjusting the  $K_{cb}$  and the corresponding  $p$ -values for each crop stage; then, the deep percolation parameters  $a_D$  and  $b_D$  of the Liu et al. [64] parametric functions; in a third step,  $Z_e$ , TEW, and REW; and lastly, the CN value. Model calibration then moved to using E2 SWC data, where  $K_{cb}$  and the corresponding  $p$ -values for each crop stage were modified while maintaining all other

parameters constant. Model calibration was considered terminated when the best fit was achieved in both E1.1 (2011) and E2.3 (2016) plots and the errors of prediction did not change from an iteration to the next. If that goal was not achieved at the end of the first trial and error cycle, the calibration process restarted again. Validation was then performed by comparing measured and simulated SWCs in the remaining E1 and E2 plots using the previously calibrated model parameters. Two different calibration processes were used for E1 and E2 data because canopies were different in terms of fractions of shaded area and crop height and because it is known that  $K_{cb}$  depends upon  $f_c$  and  $h$ .

The goodness-of-fit indicators used to evaluate model performance were those proposed by Pereira et al. [72] to compare observed ( $O_i$ ) and predicted ( $P_i$ ) values: the regression coefficient of the linear regression through the origin ( $b_0$ ), the coefficient of determination ( $R^2$ ) of the ordinary least-squares regression between observed and predicted values, the root mean square error (RMSE), the ratio of the RMSE to the standard deviation of the observed data (NRMSE), the percent bias of estimation (PBIAS), and the modeling efficiency (NSE), i.e., the residual variance compared to the measured data variance. The use and usefulness of these indicators have been discussed by many researchers [73–75].  $b_0$  equal to 1 indicates that the predicted values are statistically identical to the measurements.  $R^2$  values close to 1 indicate that the model is capable of explaining the variance of the observations. RMSE and NRMSE values close to zero show that estimation errors are small and model predictions are good [74]. PBIAS values close to zero describe accurate model simulations, while negative or positive values indicate over- or under-estimation bias, respectively. NSE values close to 1 indicate that the residuals' variance is much smaller than the observed data variance; hence, the model predictions are good. When  $NSE < 0$ , the observed mean is a better indicator than the model-predicted values [73].

### 3. Results and Discussion

#### 3.1. Parametrization of the SIMDualKc Model

Table 7 presents the model parameters calibrated for both irrigation experiments performed in the citrus orchard. Parameters relative to E1 were obtained with data from the E1.1 (2011) treatment. Parameters relative to E2 were found using data from the E2.3 (2016) treatment. These parameters were then validated with data collected in the remaining treatments of the respective experiments. The parameters related to soil properties were, naturally, the same among experiments. Only those related to the crop differed.

**Table 7.** Default and calibrated model parameters.

Parameter	Experiment 1 (2007–2011)		Experiment 2 (2015–2017)	
	Default	Calibration	Default	Calibration
$K_{cb}$ non-growing	-	0.54	-	0.64
$K_{cb}$ ini	0.55	0.54	0.65	0.64
$K_{cb}$ mid	0.55	0.55	0.65	0.64
$K_{cb}$ end	0.55	0.54	0.65	0.64
$p_{ini}$	0.50	0.60	0.50	0.60
$p_{mid}$	0.50	0.60	0.50	0.60
$p_{end}$	0.50	0.60	0.50	0.60
TEW (mm)	40	40	40	40
REW (mm)	8	8	8	8
$Z_e$ (m)	0.10	0.10	0.10	0.10
$a_D$	-	490	-	490
$b_D$	-0.0173	-0.02	-0.0173	-0.02
CN	70	80	70	80

Note:  $K_{cb}$ , basal crop coefficient for the initial ( $K_{cb}$  ini), mid-season ( $K_{cb}$  mid), and end-of-season stages ( $K_{cb}$  end);  $p$ , depletion fraction for no stress during the initial ( $p_{ini}$ ), mid-season ( $p_{mid}$ ), and end-of-season stages ( $p_{end}$ ); TEW, total evaporable water; REW, readily evaporable water;  $Z_e$ , depth of the soil evaporation layer;  $a_D$  and  $b_D$ , parameters of deep percolation; CN, curve number.

In E1, the calibrated  $K_{cb}$  values for the initial, mid-season, and end-of-season stages were 0.54, 0.55, and 0.54, respectively. In E2,  $K_{cb\ ini}$ ,  $K_{cb\ mid}$ , and  $K_{cb\ end}$  were calibrated to 0.64, 0.64, and 0.64, respectively. These values were equal or close to the default settings, which were defined according to Rallo et al. [38] and considering that the  $f_c$  and  $h$  values observed during the different experimental seasons were approximately equal for the treatments of the E1 and E2 experiments (Table 6). When the trees were 10–14 years old, the  $f_c$  values ranged from 0.46 to 0.50, while at 18–20 years old, trees had larger  $h$  values, and the canopies were larger, with  $f_c$  values from 0.75 to 0.77. Higher  $f_c$  and  $h$  values corresponded to a larger leaf area and higher transpiration and  $K_{cb}$  values.

The calibrated  $K_{cb\ mid}$  value for the 10–14-year-old clementine trees (E1) approached the  $K_{cb\ mid}$  of 0.56 tabled in Rallo et al. [28] for mature orange trees with an  $f_c$  of 0.40. The calibrated  $K_{cb\ mid}$  was also close to the  $K_{cb\ mid}$  of 0.55 reported by Er-Raki et al. [31] for 13-year-old orange trees, but with a larger  $f_c$  of 0.70. More notorious differences were observed when comparing our values with the  $K_{cb\ mid}$  of 0.50 reported by Er-Raki et al. [31] for 15-year-old orange trees with an  $f_c$  of 0.30, or the  $K_{cb\ mid}$  of 0.80 reported by Taylor et al. [26] for 14-year-old orange trees having an  $f_c$  of 0.88. The calibrated  $K_{cb\ mid}$  value for 18–20 years old clementine trees (E2), which averaged 0.64 for an  $f_c = 0.75$ , was lower than the  $K_{cb\ mid}$  of 0.75–0.78 reported by Jafari et al. [29] for 25-year-old orange trees having an  $f_c$  of 0.85. Differences in  $K_{cb}$  result from the impacts of  $f_c$  and  $h$  as used in the A&P approach described in Section 2.2. The  $K_{cb}$  during the non-growing season ( $K_{cb\ ngro}$ ) was set equal to  $K_{cb\ ini}$  due to the similarity of environmental conditions.

The calibrated fractions of soil water depletion for no-stress  $p_{ini}$ ,  $p_{mid}$ , and  $p_{end}$  values were set to 0.60 for all growing stages, showing an increase relative to those proposed by Allen et al. [37] for citrus trees. No noticeable differences were found in terms of tolerance to water stress produced by different fractions of water depletion regarding the various crop development stages and tree age.

The calibrated values of  $Z_e$ , TEW, and REW, as well as of  $a_D$  and  $b_D$ , describe the hydraulic properties of the clay soil in the studied area, approaching those set in Darouich et al. [52,53] for the nearby fields. The most relevant difference was noticed for the TEW, the calibrated value of which was higher than that in those studies. Lastly, the curve number also approached that set in Darouich et al. [52,53] but with the necessary adjustment to a fine-textured soil covered with a permanent tree crop.

### 3.2. Performance of the SIMDualKc Model

The comparison between the SIMDualKc-simulated soil water content (SWC) and the daily measured SWC for the years 2007–2011 relative to experiment E1 is presented in Figure 4. The figure also includes the depths and dates of irrigation and rainfall events. Experiment E1 aimed to assess the impacts of the irrigation method on soil water dynamics, with all treatments receiving the same amount of water at the same dates. Thus, the applied depths were inadequately high for some of the referred methods, which negatively impacted the soil water balance (Section 3.4). This was particularly relevant in the E1.1 drip treatment. For all treatments, the measured SWC values were generally between  $\theta_{FC}$  and  $\theta_p$  during the five studied growing seasons, occasionally raising above, namely, when rainfall added to irrigation events. In the E1.1 experiment, during the irrigation seasons, the SWC values were closer to  $\theta_{FC}$  than those of other treatments, which then led to higher percolation after rainfall events. This behavior may be explained by the different  $f_w$  values relative to each irrigation method, which ranged from 0.25 in drip irrigation to 0.70 in ring basins, with the larger wetted surface corresponding to less infiltration by the unit area, thus promoting lower SWC in the case of ring basin and higher SWC in the case of dripping.

The statistical indicators used to evaluate the goodness-of-fit between simulated and measured SWC values in E1 are presented in Table 8. The E1.1 (2011) treatment was selected for calibration, with the SIMDualKc model performing well when simulating the SWC. Regression coefficient  $b_0$  was close to the 1.0 target, indicating that the simulated values

were close to the observed ones. The value of  $R^2$  was relatively high (0.78), showing that the model could explain most of the variability of the observed data. The errors of the estimates were small, resulting in  $RMSE = 0.001 \text{ m}^3 \text{ m}^{-3}$  and  $NRMSE = 0.002$ . In agreement with  $b_0$ , the PBIAS was small, with no particular over- or under-estimation trend in simulating the measured data. Lastly, the EF value was also relatively high (0.70), indicating that the variance of the residuals was smaller than the measured data variance.

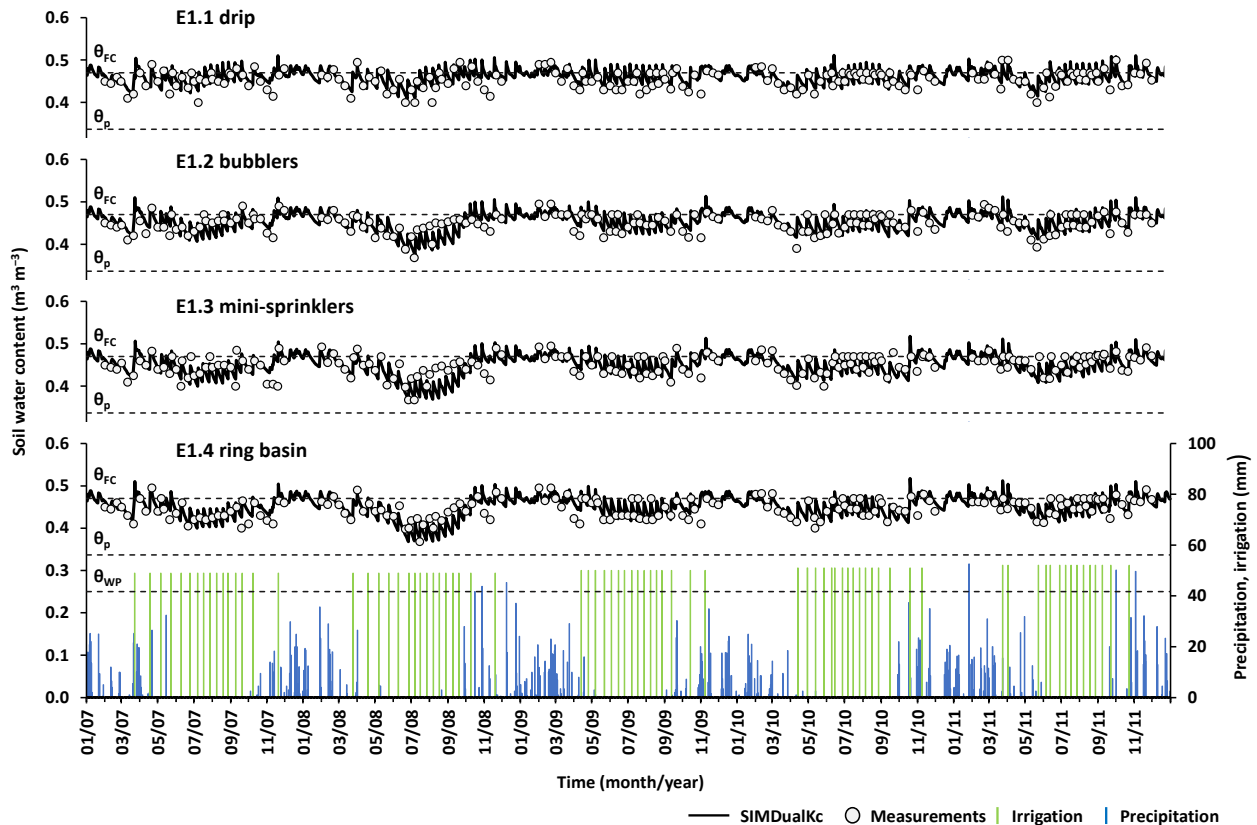


**Figure 4.** Measured and simulated soil water contents in the E1.1 drip, E1.2 bubbler, E1.3 micro-sprinkling, and E1.4 ring-basin treatments during the 2007–2011 growing seasons ( $\theta_{FC}$ ,  $\theta_{WP}$ , and  $\theta_p$  refer to soil water contents at field capacity, wilting point, and depletion fraction for no stress, respectively).

The goodness-of-fit indicators relative to the validation were similar to the calibration indicators and thus also quite good. All 23 data sets had a  $b_0$  close to 1.0, ranging from 0.98 to 1.02; most  $R^2$  were larger than 0.60; errors were small, with the RMSE generally not exceeding  $0.002 \text{ m}^3 \text{ m}^{-3}$  and the NRMSE generally not larger than 0.004; the PBIAS was small, ranging from  $-2.04\%$  and  $+1.84\%$  and thus not showing trends for over- or under-estimating the SWC for none of the four irrigation methods considered. In addition, the NSE was always positive, indicating that the variance of residuals was clearly smaller than the variance of SWC observations for all sets. This means that the SIMDualKc model was able to simulate the SWC of the orchard using the dual  $K_c$  approach for all the irrigation methods adopted locally and various irrigation water applications, either near the optimal or highly exceeding the required depths.

The comparison between the SIMDualKc-simulated SWC and the daily measured SWC values relative to the E2 treatments performed in the years 2015–2017, all referring to drip irrigation, are presented in Figure 5. The dates and depths of irrigation and rainfall events are included in the same figure. The SWC values in the E2 plots, similarly for E1 reported above (Figure 4), were generally between the  $\theta_{FC}$  and  $\theta_p$  values for most of the simulated period. However, the irrigation water depths applied were smaller than in the

E1 experiment and were not enough to maintain SWC values close to  $\theta_{FC}$ , and the SWC in the E2.1 plot dropped below  $\theta_p$  for some extended dry summer periods.

**Table 8.** Goodness-of-fit indicators for the adjustment between measured and simulated values.

Year	Treatment	$b_0$ (-)	$R^2$ (-)	RMSE ( $m^3 m^{-3}$ )	NRMSE (-)	PBIAS (%)	NSE (-)
Experiment 1							
2007	E1.1	1.02	0.60	0.002	0.004	-1.99	0.41
	E1.2	1.01	0.54	0.001	0.003	-0.75	0.52
	E1.3	1.01	0.47	0.002	0.004	-0.89	0.44
	E1.4	1.02	0.69	0.001	0.003	-1.74	0.57
2008	E1.1	1.02	0.62	0.002	0.004	-1.77	0.52
	E1.2	0.99	0.55	0.002	0.006	0.69	0.24
	E1.3	0.98	0.55	0.004	0.008	1.84	0.32
	E1.4	0.99	0.63	0.002	0.006	1.22	0.40
2009	E1.1	1.02	0.60	0.002	0.004	-2.04	0.39
	E1.2	1.01	0.50	0.002	0.004	-1.01	0.44
	E1.3	1.00	0.59	0.001	0.003	-0.60	0.57
	E1.4	1.02	0.52	0.002	0.005	-1.78	0.41
2010	E1.1	1.01	0.57	0.001	0.002	-1.41	0.39
	E1.2	1.01	0.53	0.001	0.003	-1.06	0.46
	E1.3	1.00	0.65	0.001	0.002	-0.11	0.64
	E1.4	1.00	0.61	0.001	0.002	-0.18	0.60
2011	E1.1, calibr.	1.01	0.78	0.001	0.002	-1.37	0.70
	E1.2	1.01	0.77	0.001	0.002	-1.21	0.71
	E1.3	1.00	0.62	0.001	0.002	-0.06	0.52
	E1.4	1.00	0.60	0.001	0.002	-0.26	0.48
Experiment 2							
2015	E2.1	0.96	0.89	0.004	0.011	4.54	0.72
	E2.2	1.00	0.71	0.002	0.005	0.32	0.42
	E2.3	1.00	0.78	0.002	0.006	0.44	0.75
2016	E2.1	0.99	0.93	0.002	0.005	1.69	0.82
	E2.2	0.99	0.80	0.001	0.003	0.73	0.79
	E2.3, calib.	1.00	0.82	0.002	0.004	0.26	0.81
2017	E2.1	0.99	0.92	0.002	0.004	0.85	0.83
	E2.2	1.03	0.79	0.002	0.005	-2.57	0.64
	E2.3	1.01	0.85	0.001	0.003	-1.52	0.80

Note:  $b_0$ , regression coefficient;  $R^2$ , coefficient of determination; RMSE, root mean square error; NRMSE, ratio of the RMSE to the standard deviation of observed data; PBIAS, percent bias; NSE, model efficiency.

The SIMDualKc model performed quite well when simulating SWC for the nine data sets of the E2 plots for calibration (E2.3; 2016) and validation (all other data sets). These simulations produced comparable or better goodness-of-fit indicators than those reported for E1 (Table 8). The indicators consisted of a  $b_0$  close to 1.0, ranging from 0.96 to 1.03, thus not identifying a trend for upper- or under-estimating the SWC; the  $R^2$  values ranged from 0.71 to 0.92, thus indicating that the model largely explained the variance of the SWC; the PBIAS was small, ranging from -2.54% and +4.64%, thus confirming that no heavy trends occurred when estimating the SWC for all three irrigation schedules considered; errors were small, with only one RMSE value exceeding  $0.002 m^3 m^{-3}$  and one NRMSE value larger than 0.006; finally, the NSE were generally larger than 0.70, thus indicating that the variance of the residuals was definitely smaller than the variance of the SWC observations for all sets. This means, as for E1 experiments, that the SIMDualKc model was able to simulate the SWC of the orchard using the dual  $K_c$  approach for all the drip-irrigation schedules used, including when over-irrigation was practiced.

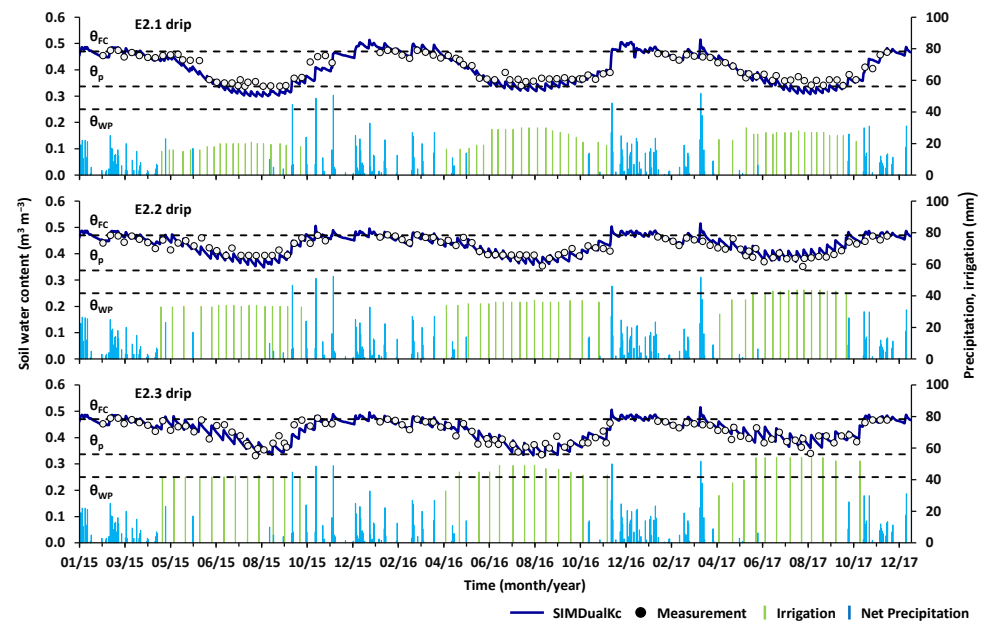


**Figure 5.** Measured and simulated soil water contents in the E2 treatments during the 2015–2017 growing seasons ( $\theta_{FC}$ ,  $\theta_{WP}$ , and  $\theta_p$  refer to soil water contents at field capacity, wilting point, and depletion fraction for no stress, respectively).

The reported goodness-of-fit indicators for the E1 and E2 experiments are within the ranges of values reported in the literature for the SIMDualKc simulations of perennial crops for vineyards [67,76–78], peach orchards [42], and olive groves [66,79,80]. They are also similar to those reported by Darouich et al. [52,53] for horticultural crops grown in the same edapho-climatic conditions in the Akkar plain. As such, the obtained results were considered adequate for the analysis reported below.

### 3.3. SIMDualKc vs. A&P Approach

The parameterization of the A&P approach (Section 2.2.2), which is a novel approach to estimate the actual  $K_c$ , was performed by applying Equations (11–13) using the available average values of  $f_c$  and  $h$  observed during the clementine growing seasons (Table 6). The  $M_L$  value was set to 1.7, following Pereira et al. [71]. Reduction factor  $F_r$  was analyzed considering the range of proposed values based on crop density and height in Pereira et al. [71]. For Experiment 1 (2007–2011), an  $F_r$  of 0.55 was adopted for all crop stages, which corresponds to the upper value suggested for medium density and height of citrus trees. For Experiment 2, an  $F_r$  value of 0.61 was assumed, corresponding to the central value of the proposed range for high-density and medium–high citrus trees. Naturally, these values were selected after testing the lower, central, and upper values of  $F_r$  in the proposed range and comparing the resulting  $K_{cb\ A\&P}$  with the calibrated  $K_{cb}$  with SIMDualKc (Table 7). Table 9 presents the  $K_{cb\ A\&P}$  values obtained for the different growing seasons of Experiments 1 and 2.

In Experiment 1, the  $K_{cb\ A\&P}$  values were only slightly smaller than the model-derived  $K_{cb}$  for all crop stages (Table 7). The exception refers to the case when  $f_c$  and  $h$  values were the highest. In Experiment 2, the  $K_{cb\ A\&P}$  values were quite close to the model-derived  $K_{cb}$  values, with the largest differences being found for 2017. The variability of  $K_{cb\ A\&P}$  was in agreement with that of the  $f_c$  and  $h$  values used in their computation.

**Table 9.**  $K_{cb}$  values estimated with the A&P approach.

Season	$K_{cb}$ A&P ini	$K_{cb}$ A&P mid	$K_{cb}$ A&P end	Season	$K_{cb}$ A&P ini	$K_{cb}$ A&P mid	$K_{cb}$ A&P end
Experiment 1				Experiment 2			
2007	0.50	0.51	0.51	2015	0.63	0.63	0.65
2008	0.53	0.53	0.52	2016	0.65	0.65	0.67
2009	0.52	0.54	0.52	2017	0.67	0.67	0.66
2010	0.52	0.55	0.54				
2011	0.53	0.54	0.53				

Note: Basal crop coefficients for the initial ( $K_{cb}$  A&P ini), mid-season ( $K_{cb}$  A&P mid), and end-of-season stages ( $K_{cb}$  A&P end).

The  $K_{cb}$  A&P values were tested as alternatives to the calibrated  $K_{cb}$  values in the computation of the soil water balance using SIMDualKc. Such testing approach is novel. The goodness-of-fit indicators relative to the fitting of the measured SWC by the simulated one are presented in Table 10. These values compared well with those reported in Table 8 when the calibrated  $K_{cb}$  were used. However, slight differences occurred, e.g., for plots E1.4 (2007), E1.3 (2008), and E2.3 (2017), there were smaller  $R^2$  and NSE indicators when using the A&P approach, while in plots E1.2 (2007), E1.3 (2007), and E2.2 (2015), it was the other way around. The A&P approach may, thus, be considered a good alternative to the model calibration of  $K_{cb}$  values to be used in scenario analysis.

**Table 10.** Goodness-of-fit indicators for the adjustment between measured and simulated soil water content values using the A&P approach.

Year	Treatment	$b_0$ (-)	$R^2$ (-)	RMSE ( $m^3 m^{-3}$ )	NRMSE (-)	PBIAS (%)	NSE (-)
Experiment 1							
2007	E1.1	1.02	0.59	0.002	0.004	-2.40	0.31
	E1.2	1.02	0.68	0.001	0.003	-1.64	0.54
	E1.3	1.02	0.55	0.002	0.005	-1.98	0.40
	E1.4	1.03	0.66	0.002	0.004	-2.94	0.31
2008	E1.1	1.02	0.63	0.002	0.005	-2.20	0.48
	E1.2	1.00	0.57	0.002	0.004	-0.47	0.33
	E1.3	0.99	0.47	0.003	0.006	0.66	0.27
	E1.4	1.00	0.65	0.002	0.004	-0.20	0.57
2009	E1.1	1.02	0.60	0.002	0.004	-2.10	0.37
	E1.2	1.01	0.51	0.002	0.004	-1.21	0.44
	E1.3	1.01	0.59	0.001	0.003	-0.79	0.56
	E1.4	1.02	0.53	0.002	0.005	-2.01	0.39
2010	E1.1	1.01	0.56	0.001	0.003	-1.48	0.37
	E1.2	1.01	0.52	0.001	0.003	-1.18	0.44
	E1.3	1.00	0.63	0.001	0.002	-0.18	0.63
	E1.4	1.00	0.61	0.001	0.002	-0.28	0.60
2011	E1.1	1.01	0.77	0.001	0.002	-1.47	0.68
	E1.2	1.01	0.77	0.001	0.002	-1.36	0.69
	E1.3	1.00	0.62	0.001	0.002	-0.27	0.54
	E1.4	1.00	0.60	0.001	0.002	-0.41	0.49
Experiment 2							
2015	E2.1	0.96	0.89	0.004	0.010	4.14	0.74
	E2.2	1.00	0.70	0.002	0.005	-0.40	0.48
	E2.3	1.00	0.79	0.002	0.005	-0.34	0.78
2016	E2.1	0.98	0.94	0.002	0.006	2.02	0.81
	E2.2	0.98	0.82	0.001	0.003	1.77	0.75
	E2.3	0.99	0.82	0.002	0.005	1.20	0.79
2017	E2.1	0.98	0.92	0.002	0.006	1.98	0.77
	E2.2	1.01	0.82	0.002	0.005	-0.51	0.69
	E2.3	0.99	0.84	0.002	0.004	0.84	0.71

### 3.4. Dynamics of Crop Coefficients and the Soil Water Balance

Table 11 presents the soil water balance computed by SIMDualKc for the clementine orchard during the 2007–2011 growing seasons (Experiment 1). Seasonal irrigation depths were very homogeneous throughout the seasons, ranging from 780 mm in 2011 to 816 mm in 2010. In addition, seasonal net precipitation values were relatively high and varied between 612 mm in 2010 and 902 mm in 2011. Water inputs deeply contrasted with annual  $T_c$  values, which were relatively constant and ranged from 644 mm in 2007 to 680 mm in 2010. Thus, the first conclusion is that the experiments were conducted with excess water application. Excessive rainfall mostly converted into runoff and excess irrigation turned into deep percolation. Therefore, the DP and RO annual values were uncommonly high. The variation in the SWC at the annual scale was very small because the water extracted from the soil was replaced by the next wetting through rainfall or irrigation. Thus, soil water storage did not play a seasonal buffer role as it could be expected when irrigating in a dry area.

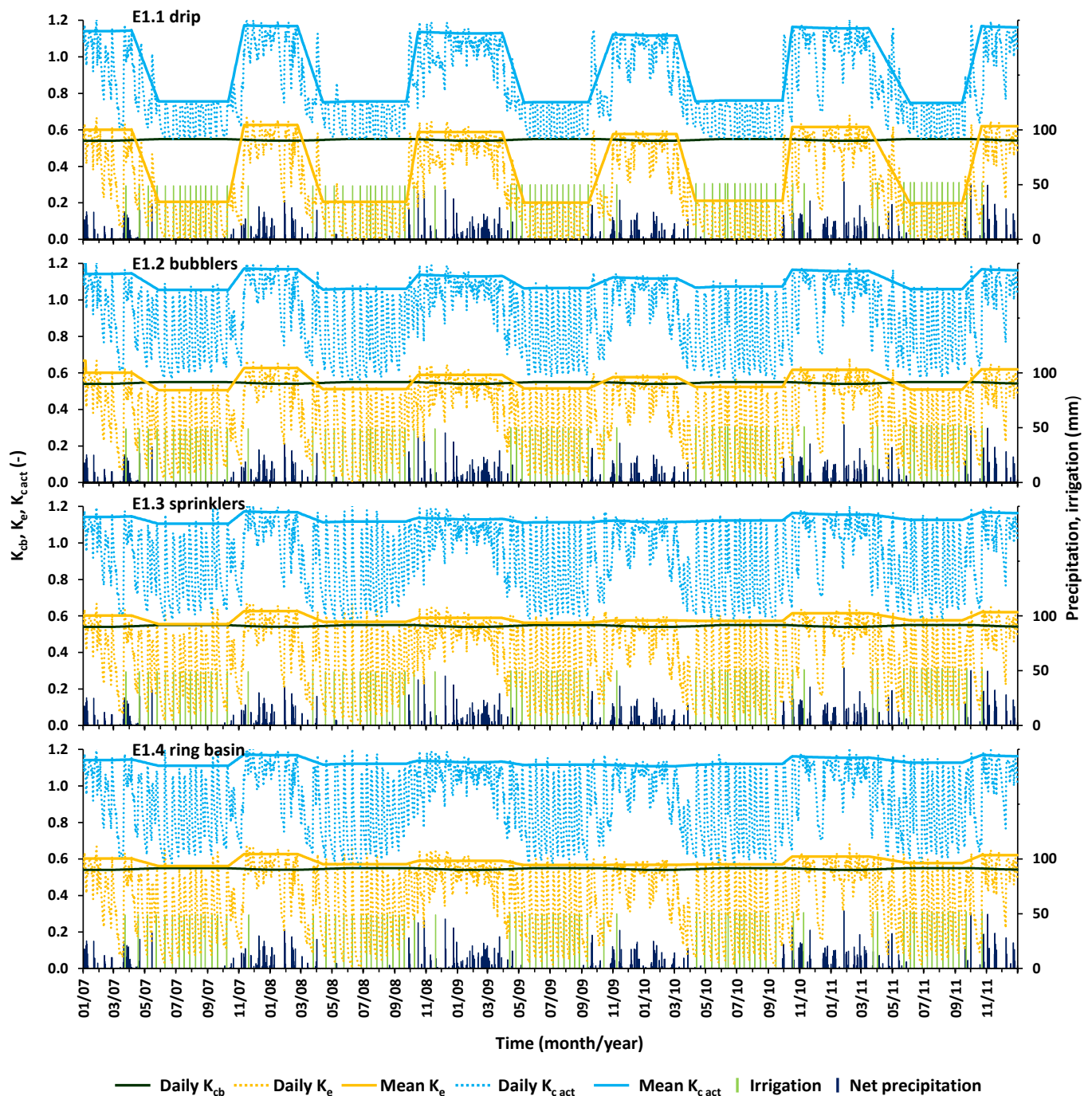
**Table 11.** Components of the annual water balance during E1 growing seasons.

Year	Treatment	Inputs (mm)			Outputs (mm)				
		I	Net P	$\Delta$ SW	$T_c$	$T_{c\ act}$	$E_s$	DP	RO
2007	E1.1	784	663	−2	644	644	247	555	252
	E1.2	784	662	−2	644	644	355	446	253
	E1.3	784	661	−2	644	644	379	421	254
	E1.4	784	661	−2	644	644	380	421	254
2008	E1.1	784	629	−20	666	666	242	487	164
	E1.2	784	629	−20	666	666	360	369	164
	E1.3	784	629	−20	666	666	384	345	164
	E1.4	784	629	−20	666	666	384	345	164
2009	E1.1	800	803	7	653	653	255	699	216
	E1.2	800	802	7	653	653	382	570	218
	E1.3	800	802	7	653	653	399	553	218
	E1.4	800	801	7	653	653	399	553	218
2010	E1.1	816	612	1	680	680	237	514	151
	E1.2	816	612	1	680	680	360	389	152
	E1.3	816	612	1	680	680	377	373	151
	E1.4	816	612	1	680	680	378	372	151
2011	E1.1	780	902	0	652	652	283	744	169
	E1.2	780	902	0	652	652	392	635	169
	E1.3	780	902	0	652	652	412	615	169
	E1.4	780	902	0	652	652	413	613	169

Note: I, irrigation; P, precipitation;  $\Delta$ SW, variation in soil water storage;  $T_c$ , potential crop transpiration;  $T_{c\ act}$ , actual soil transpiration;  $E_s$ , soil evaporation; DP, deep percolation; RO, runoff.

The potential and actual transpiration were equal because the crop was never submitted to water stress. Soil evaporation was generally high, but the drip-irrigated experiment consistently showed a smaller value relative to other methods, with differences larger than 100 mm, because the wetted ground area, from where soil evaporation originated, was the smallest.

Figure 6 shows the dynamics of the potential basal crop coefficients ( $K_{cb}$ ), the soil evaporation coefficients ( $K_e$ ), and the actual crop coefficient ( $K_{C\ act} = K_{cb\ act} + K_e$ ) during the five growing seasons (2007–2011). Because the crop was not stressed, the actual basal crop coefficient ( $K_{cb\ act}$ ) curves were always coincident with the  $K_{cb}$  curves for all cases. As a result,  $T_{c\ act}$  values always matched the potential ones. The greatest contrast among the E1 treatments was found in the  $K_e$  dynamics, because the wetted and exposed soil fractions were much smaller than for the other methods. Thus,  $K_e$  during mid-season was much smaller for dripping, also resulting in a much smaller  $K_{C\ act\ mid}$ .



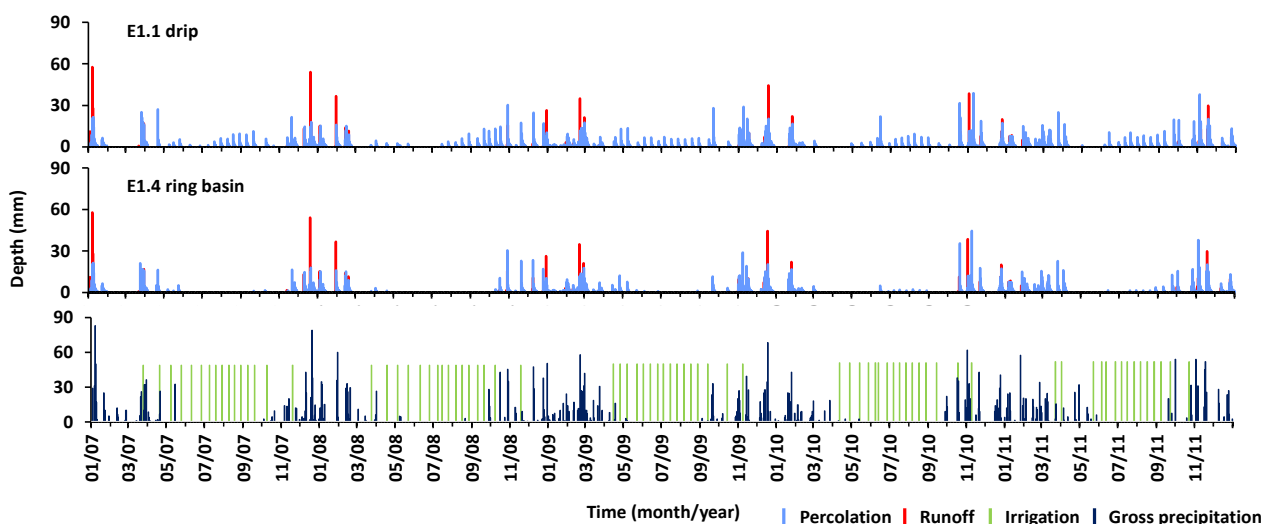
**Figure 6.** Seasonal variation in the standard (non-stressed) basal crop coefficient ( $K_{cb}$ ), the actual basal crop coefficient ( $K_{cb_{act}}$ ), and the evaporation coefficient ( $K_e$ ) in E1.1 drip, E1.2 bubbler, E1.3 micro-sprinkling, and E1.4 ring-basin plots during the 2007–2011 growing seasons, including the respective data on irrigation and precipitation.

Figure 6 describes numerous  $K_e$  peaks that represent soil evaporation responses to rainfall and irrigation wettings for all the different crop stages and seasons. The  $K_e$  responses to rainfall events were identical among treatments, producing high peaks as the entire soil surface was wetted ( $f_w = 1$ ). The  $K_e$  peaks in the E1.1 drip plots were smaller, as the soil wetted fraction was also much smaller ( $f_w = 0.25$ ).

Based on the referred dynamics, the seasonal  $E_s$  values were lower in the plots irrigated by dripping, ranging from 237 to 283 mm, and higher in those irrigated by ring basins,

varying from 378 to 413 mm. As also shown in Table 11, the deep percolation values were expectably high throughout the years considering the high seasonal water inputs from irrigation and precipitation. Percolation was the highest in the E1.1 drip plots, ranging from 487 mm in 2008 to 744 mm in 2011. The lowest values were determined in the E1.4 ring-basin plots, varying from 345 mm to 613 mm in those same years, values that were also too high.

The differences among treatments are depicted in Figure 7, which presents the daily percolation and runoff values during the studied seasons. In the E1.1 plots, up to 61% of the seasonal percolation occurred during the irrigation season. This mainly resulted from the large irrigation depths applied per event (49–52 mm), the frequency of those events (13–15 days), the occurrence of some precipitation during the irrigation season without adjusting the irrigation schedules, and the lower soil evaporation that maintained soil moisture higher and close to  $\theta_{FC}$  (Figure 5). On the other hand, in the other plots, namely, the E1.4 basin plots, only 28%–48% of the seasonal percolation occurred during the irrigation period. The seasonal values of runoff ranged from 151 mm in 2010 to 254 mm in 2007. For all irrigation methods, runoff occurred only during the rainfall season, as depicted in Figure 7.



**Figure 7.** Daily values of percolation and runoff in E1.1 drip and E1.4 ring-basin plots during the 2007–2011 growing seasons (E1).

The soil water balance computed by SIMDualKc for the clementine orchard during the 2015–2017 growing seasons (Experiment 2) is presented in Table 12. The seasonal irrigation depths were considerably smaller in E2 than in E1, with the largest sums being applied in E2.2 (535–620 mm) and the lowest in the E2.1 (368–493 mm) treatment. Nevertheless, those seasonal depths were excessive, as it may be seen by observing the DP occurrence in Table 12, which was also due to keeping the soil wetted by irrigation most of the time. The seasonal net precipitation was similar to those observed for E1, ranging from 634 to 758 mm. The seasonal  $T_c$  values increased to values from 748 to 770 mm, in line with the highest  $K_{cb}$  values set for the E2 treatments when compared with E1 (Table 7).

In the E2.2 and E2.3 plots,  $K_{cb,act}$  always matched the potential  $K_{cb}$  values, i.e., no water stress occurred throughout the different growing seasons, as it may be also observed in Figure 8. On the other hand, in the E2.1 plots,  $K_{cb,act}$  dropped below  $K_{cb}$  when soil moisture was also below  $\theta_p$ . Clementine trees were then subjected to mild water stress ( $T_{c,act}/T_c$  reduced by 5–10%) for some extended periods, which mostly resulted from inadequate irrigation scheduling. It is known that the effects on yields are closely related to the timing and duration of irrigation events and crop physiological status, with the most critical growth stages being the flowering and fruit growth periods [30]; hence, maintaining

a mild–moderate water stress for such extended periods in E2.1 (Figure 8) ended up affecting yields.

**Table 12.** Components of the annual water balance relative to the E2 growing seasons.

Year	Treatment	Inputs (mm)				Outputs (mm)			
		I	Net P	$\Delta SW$	$T_c$	$T_{c\ act}$	$E_s$	DP	RO
2015	E2.1	368	722	−25	748	674	163	228	135
	E2.2	535	758	−23	748	748	154	369	99
	E2.3	502	720	−22	748	748	139	314	137
2016	E2.1	490	634	−8	770	704	135	272	160
	E2.2	608	634	−8	770	770	133	326	160
	E2.3	588	638	−8	770	769	115	329	156
2017	E2.1	493	673	−18	763	726	143	279	206
	E2.2	620	669	−1	763	763	134	392	210
	E2.3	590	669	−1	763	763	121	375	210

Note: I, irrigation; P, precipitation;  $\Delta SW$ , variation in soil water storage; CR, capillary rise;  $T_c$ , crop transpiration;  $T_{c\ act}$ , actual soil transpiration;  $E_s$ , soil evaporation; DP, deep percolation; RO, runoff.

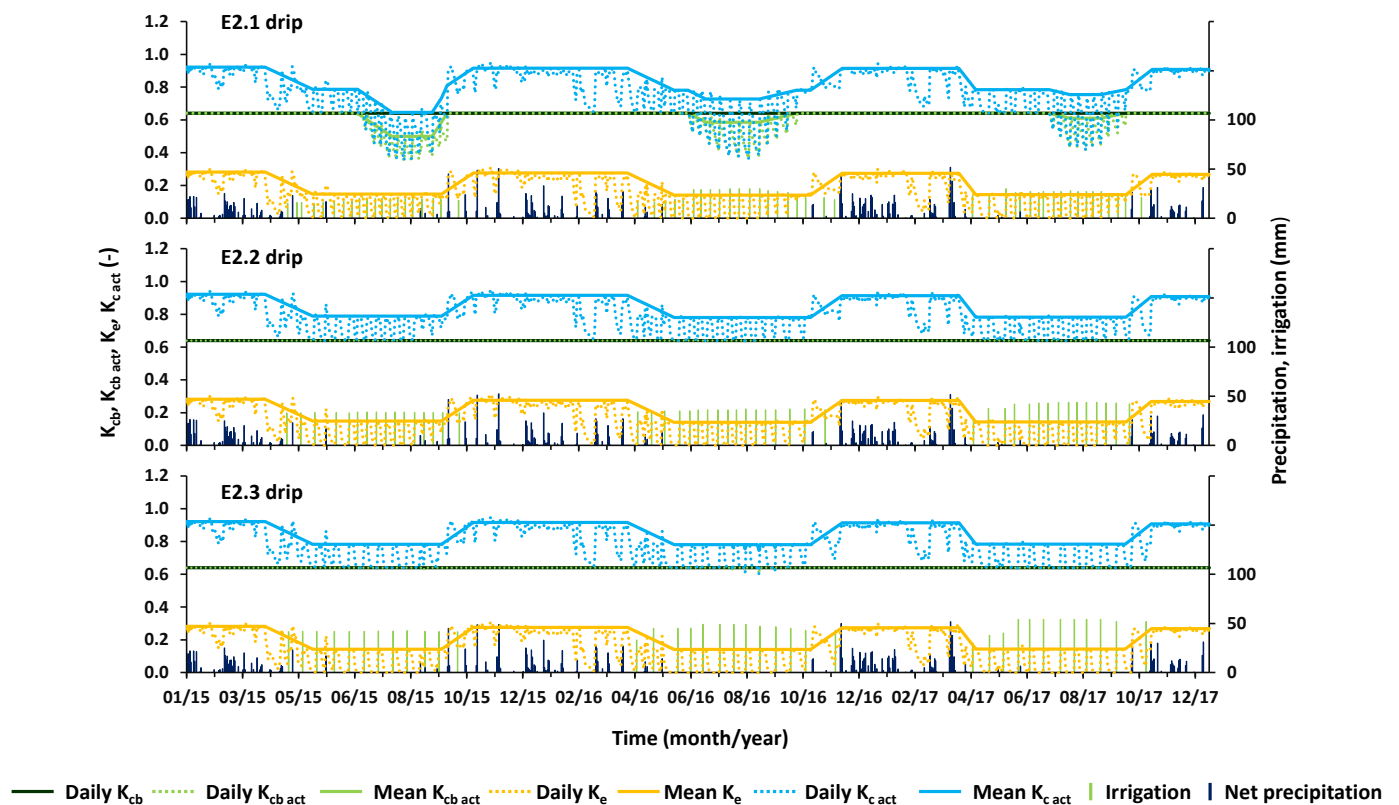


**Figure 8.** Seasonal variation in the standard (non-stressed) basal crop coefficient ( $K_{cb}$ ), the actual basal crop coefficient ( $K_{cb\ act}$ ), and the evaporation coefficient ( $K_e$ ) in E2 plots during the 2015–2017 growing seasons, including the respective data on irrigation and precipitation.

The dynamic observed for  $K_e$  in E2 (Figure 8) was similar to that reported for the E1 drip plots in Figure 6.  $K_e$  increased to maximum values in response to rainfall events, when the entire soil surface was wetted, and then dropped to minimum values when the evaporation soil layer dried out. After irrigation events,  $K_e$  also increased but less than for rainfall events, as only a small area of the soil surface was wetted by the drippers. Nevertheless, soil evaporation was considerably smaller in E2 than that in E1 plots, with maximum values from 135 to 163 mm in the E2.1 plots and minimum ones from 115 to 139 mm in the

E2.3 plots (Table 12). This was both due to smaller irrigation depths and smaller wetted and exposed fractions  $f_{ew}$  in E2 relative to E1 as the ground shaded by the trees' canopies was larger, thus limiting the energy available for soil evaporation.

The seasonal percolation and runoff were also high in E2, ranging from 228 to 392 mm and from 99 to 210 mm, respectively (Table 12). Yet, as shown in Figure 9, percolation and runoff mostly occurred during the rainfall season, thus indicating that excess irrigation was limited.

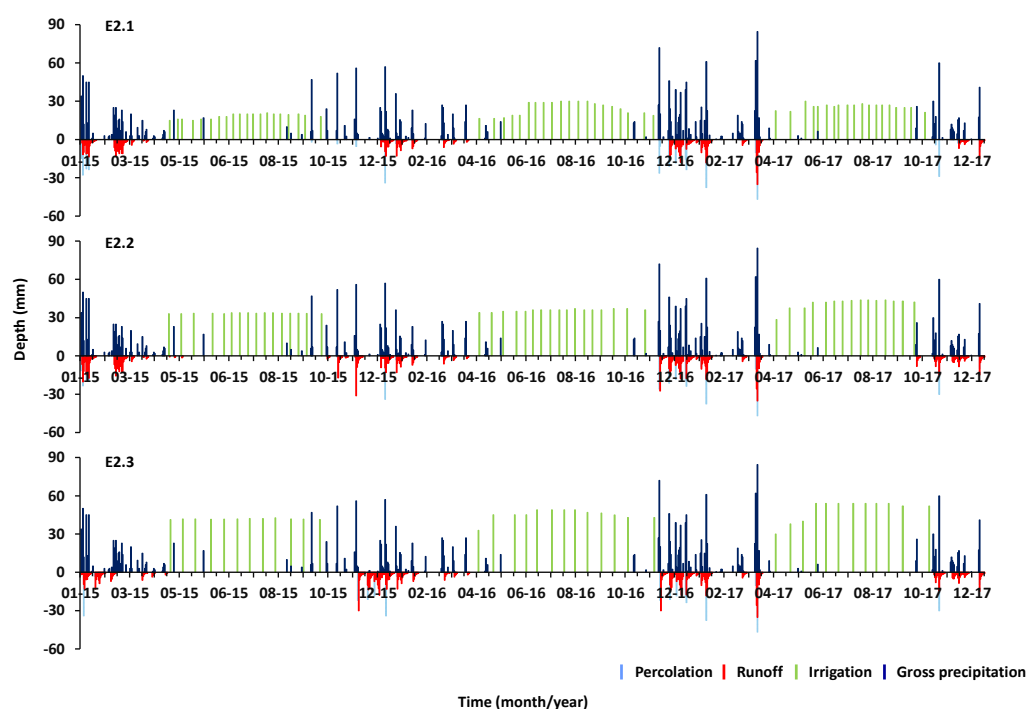


**Figure 9.** Daily values of percolation and runoff in E2 plots during the 2015–2017 growing seasons.

The  $K_c$  values computed from summing standard  $K_{cb}$  with the  $K_e$  observed during the initial, mid-season, and end-of-season stages, and the non-growing season are summarized in Table 13. The  $K_{c\ ini}$  for E1 were approximately equal to the  $K_{c\ end}$  and the  $K_c$  for the non-growing period, 1.15, when  $K_e$  averaged the same value independently of the year, since no droughts were observed and the canopies were similar. Differently,  $K_{c\ mid}$  were distinct depending upon the wetted and exposed fractions, with a smaller  $K_{c\ mid}$  in the case of drip irrigation (0.76) and larger one for the other methods (1.06–1.12). For E2, with all treatments using drip irrigation,  $K_{c\ mid}$  (0.75–0.78) were approximately equal to the  $K_{c\ mid}$  of E1.1 (0.76), also with drip irrigation, despite the standard  $K_{cb\ mid}$  being 0.54 for E1 and 0.64 for E2. Differences refer to the canopy size, particularly the fraction covered and crop height, with  $f_c$  and  $h$  in the ranges of 0.46–0.50 and 2.5–3.0 m, respectively, in the case of E1, and ranging from 0.75 to 0.77 and from 3.8 to 4.0 m in the case of E2. The impact of canopy size and crop height on  $K_c$  is well evidenced in the results (Table 13).

The computation of the soil water balance after incorporating the A&P approach in the estimate of the  $K_{cb}$  values did not alter the analysis above when comparing Tables 14 and 15 with Tables 12 and 13. The overall lower  $K_{cb\ A\&P}$  computed for Experiment 1 reduced seasonal  $T_c$  only by values from 12 (2011) to 47 (2007) mm. These reductions resulted in small differences among the other outputs of the SWB, namely, soil evaporation and deep percolation. In Experiment 2, the lower  $K_{cb\ A\&P}$  in 2015 resulted in a decrease in seasonal  $T_c$  values of 10 mm, while the 2016 and 2017 crop seasons, with slightly higher  $K_{cb\ A\&P}$ , saw their seasonal  $T_c$  values increase by values from 13 to 25 mm and corresponding reductions in  $E_s$  and DP. Therefore, the use of  $K_{cb\ A\&P}$  in the SWB was generally minor, proving it is a viable option to support irrigation management.

**Table 13.** Single crop coefficients of a clementine orchard with different canopy sizes and various irrigation methods.

Treatment	K <sub>c ini</sub>	K <sub>c mid</sub>	K <sub>c end</sub>	K <sub>c non-growing</sub>
Experiment 1, medium-size canopies				
E1.1, drip	1.14	0.76	1.15	1.15
E1.2, bubblers	1.14	1.06	1.15	1.15
E1.3, micro-sprinklers	1.14	1.12	1.15	1.15
E1.4, ring basins	1.14	1.12	1.15	1.15
Experiment 2, large-size canopies				
E2.1, drip, moderate deficit irrigation	0.92	0.75	0.91	0.91
E2.2, drip, regulated deficit irrigation	0.92	0.78	0.91	0.91
E2.3, drip, full irrigation	0.92	0.78	0.91	0.91

**Table 14.** Components of the annual water balance relative to the E1 growing seasons following the A&P approach.

Year	Treatment	Inputs				Outputs			
		I (mm)	Net P (mm)	ΔSW (mm)	T <sub>c</sub> (mm)	T <sub>c act</sub> (mm)	E <sub>s</sub> (mm)	DP (mm)	RO (mm)
2007	E1.1	784	665	−2	597	597	254	597	250
	E1.2	784	664	−2	597	597	367	484	251
	E1.3	784	663	−2	597	597	394	455	252
	E1.4	784	664	−2	597	597	395	455	251
2008	E1.1	784	629	−20	634	634	245	516	164
	E1.2	784	629	−20	634	634	368	393	164
	E1.3	784	629	−20	634	634	394	367	164
	E1.4	784	629	−20	634	634	394	367	164
2009	E1.1	800	804	7	638	638	257	712	216
	E1.2	800	802	7	638	638	385	582	217
	E1.3	800	802	7	638	638	403	564	218
	E1.4	800	802	7	638	638	403	564	218
2010	E1.1	816	613	1	675	675	238	518	151
	E1.2	816	612	1	675	675	361	393	152
	E1.3	816	613	1	675	675	379	377	151
	E1.4	816	613	1	675	675	379	376	151
2011	E1.1	780	902	0	640	640	285	754	168
	E1.2	780	902	0	640	640	395	644	168
	E1.3	780	902	0	640	640	415	624	168
	E1.4	780	902	0	640	640	417	622	168

**Table 15.** Components of the annual water balance relative to the E2 growing seasons following the A&P approach.

Year	Treatment	Inputs				Outputs			
		I (mm)	Net P (mm)	ΔSW (mm)	T <sub>c</sub> (mm)	T <sub>c act</sub> (mm)	E <sub>s</sub> (mm)	DP (mm)	RO (mm)
2015	E2.1	368	722	−27	738	671	164	230	135
	E2.2	535	758	−23	738	738	154	379	99
	E2.3	502	721	−22	738	738	139	324	137
2016	E2.1	490	634	−8	783	709	135	267	160
	E2.2	608	634	−8	783	783	133	314	160
	E2.3	588	638	−8	783	783	115	319	156
2017	E2.1	493	673	−18	798	740	142	267	205
	E2.2	620	669	−1	798	798	132	359	210
	E2.3	590	669	−1	798	798	119	342	210

#### 4. Conclusions

This study, referring to a mature orchard of clementines in a typical Mediterranean agroecosystem in the coastal plain of Syria, focused five years of assessment of crop coefficients and water use, when the training of trees led to relatively small fraction cover and height, and three years of a similar assessment, when the crop was later trained for large  $f_c$  and  $h$ . The SIMDualKc software model was used to successfully analyze the respective field data, with RMSE values below  $0.004 \text{ m}^3 \text{ m}^{-3}$  and NSE positive values up to 0.83. Differences between canopy  $f_c$  and  $h$  led us to perform specific model calibration since  $K_{cb}$  were distinct, with  $K_{cb \text{ mid}} = 0.55$  when the canopy was smaller and  $K_{cb \text{ mid}} = 0.64$  when  $f_c$  and  $h$  were larger. Using the A&P approach, via which  $K_{cb}$  were computed from  $f_c$  and  $h$ , led to  $K_{cb \text{ A\&P}}$  values similar to those obtained from calibrating the SIMDualKc model. Simulations using  $K_{cb \text{ A\&P}}$  led to similar goodness-of-fit indicators ( $\text{RMSE} \leq 0.004 \text{ m}^3 \text{ m}^{-3}$ ;  $0.27 \leq \text{NSE} \leq 0.81$ ).

Model simulations led us to conclude that the  $K_{cb}$  values were approximately constant and equal to  $K_{cb \text{ mid}}$  in both cases, since there was no stress in none of the crop seasons analyzed. On the other hand, single  $K_c$  values were larger during the rainfall periods (1.14–1.15 in E1; 0.91–0.92 in E2), which refer to the periods comprising the end-of-season, the non-growing season, and the initial crop stage. This is likely due to the fact that soil evaporation was greater during the rainy periods, while the mid-season period was dry. Therefore, the  $K_c$  values resulted larger for the orchard with a smaller  $f_c$ , because the wetted ground surface and that exposed to radiation were larger. During mid-season (dry season), the  $K_c$  values in the drip-irrigation plots (0.75–0.76) were comparatively lower than those in plots irrigated by other pressurized or surface methods (0.78–1.12). Differences among irrigation methods resulted in different  $K_c$ , because drip irrigation created smaller wetted and exposed soil fractions.

The soil water balance demonstrated that excess water was applied in the set with smaller canopies. This problem was not observed in the second data set. The results for the soil water balance using  $K_{cb \text{ A\&P}}$  led to a partition of SWB outputs quite similar to that obtained when using the  $K_{cb}$  values obtained with the model. Thus, we could confirm the assumption that using the A&P approach is appropriate and precise enough to develop irrigation scheduling in practice using observed actual  $f_c$  and  $h$  and thus the actual crop coefficients. A companion paper devoted to developing and accessing irrigation management alternatives for citrus irrigation in Syria shall follow the current one.

**Author Contributions:** Conceptualization, H.D. and R.K.; methodology, H.D. and R.K.; software, H.D.; validation, T.B.R.; formal analysis, H.D.; investigation, H.D., R.K. and A.M.; resources, R.K. and A.M.; data curation, R.K.; writing—original draft preparation, H.D. and T.B.R.; writing—review and editing, L.S.P.; supervision, T.B.R. and L.S.P.; project administration, R.K.; funding acquisition, R.K. All authors have read and agreed to the published version of the manuscript.

**Funding:** This research project was funded by FCT/MCTES (PIDDAC) through project LARSyS-FCT Pluriannual funding 2020–2023 (UIDB/50009/2020). H. Darouich and T.B. Ramos were supported by contracts CEECIND/01153/2017 and CEECIND/01152/2017, respectively.

**Institutional Review Board Statement:** Not applicable.

**Informed Consent Statement:** Not applicable.

**Data Availability Statement:** The soil moisture data presented in this study may be available upon request from the corresponding author.

**Conflicts of Interest:** The authors declare no conflict of interest.

## References

- Langgut, D. The citrus route revealed: From southeast Asia into the Mediterranean. *HortScience* **2017**, *52*, 814–822. [CrossRef]
- Matheyambath, A.C.; Padmanabhan, P.; Paliyath, G. Citrus Fruits. In *Encyclopedia of Food and Health*; Caballero, B., Finglas, P.M., Toldrá, F., Eds.; Academic Press: Cambridge, MA, USA, 2016; pp. 136–140. [CrossRef]
- Lacirignola, C.; D’Onghia, A.M. The Mediterranean citriculture: Productions and perspectives. In *Citrus Tristeza Virus and Toxoptera Citricidus: A Serious Threat to the Mediterranean Citrus Industry*; D’Onghia, A.M., Djelouah, K., Roistacher, C.N., Eds.; Options Méditerranéennes: Série B. Etudes et Recherches; n. 65; CIHEAM: Bari, Italy, 2009; pp. 13–17.
- Food and Agriculture Organization of the United Nations. Statistics. Available online: <https://www.fao.org/statistics/en/> (accessed on 21 January 2022).
- Westlake, M. The citrus sub-sector. Syrian agriculture at the crossroads. In *Syrian Agriculture at the Crossroads, FAO Agricultural Policy and Economic Development Series No. 8*; Fiorillo, C., Vercueil, J., Eds.; Food and Agriculture Organization of the United Nations: Rome, Italy, 2003; Chapter 8; pp. 193–216.
- Wattenbach, H. *Farming Systems of the Syrian Arab Republic*; FAO Project GCP/SYR/006/ITA; The National Agricultural Policy Center (NAPC): Damascus, Syria, 2006.
- Central Bureau of Statistics. Agriculture, Chapter 4., Tables 7 and 10, Damascus, Syria. Available online: <http://cbssyr.sy/index-EN.htm> (accessed on 28 December 2021).
- Oweis, T.; Rodrigues, P.N.; Pereira, L.S. Simulation of supplemental irrigation strategies for wheat in Near East to cope with water scarcity. In *Tools for Drought Mitigation in Mediterranean Regions*; Rossi, G., Cancelliere, A., Pereira, L.S., Oweis, T., Shatanawi, M., Zairi, A., Eds.; Kluwer: Dordrecht, The Netherlands, 2003; pp. 259–272. [CrossRef]
- Varela-Ortega, C.; Sagardoy, J.A. Irrigation water policies in Syria: Current developments and future options. In *Syrian Agriculture at the Crossroads*; Fiorillo, C., Vercueil, J., Eds.; FAO Agricultural Policy and Economic Development Series No. 8; Food and Agriculture Organization of the United Nations: Rome, Italy, 2003; Chapter 13; pp. 335–360.
- Sadiddin, A. An assessment of policy impact on agricultural water use in the northeast of Syria. *Environ. Dev. Sustain.* **2013**, *2*, 74–105. [CrossRef]
- Mourad, K.A.; Alshihabi, O. Assessment of future Syrian water resources supply and demand by the WEAP model. *Hydrol. Sci. J.* **2016**, *61*, 393–401. [CrossRef]
- Abou Zakhem, B.; Al Ain, F.; Hafez, R. Assessment of field water budget components for increasing water productivity under drip irrigation in arid and semiarid areas, Syria. *Irrig. Drain.* **2019**, *68*, 452–463. [CrossRef]
- Fader, M.; Shi, S.; von Bloh, W.; Bondeau, A.; Cramer, W. Mediterranean irrigation under climate change: More efficient irrigation needed to compensate increases in irrigation water requirements. *Hydrol. Earth Syst. Sci. Discuss.* **2016**, *20*, 953–973. [CrossRef]
- Darouich, H.; Gonçalves, J.M.; Muga, A.; Pereira, L.S. Water saving vs. farm economics in cotton surface irrigation: An application of multicriteria analysis. *Agric. Water Manag.* **2012**, *115*, 223–231. [CrossRef]
- Darouich, H.; Pedras, C.M.G.; Gonçalves, J.M.; Pereira, L.S. Drip vs. surface irrigation: A comparison focusing water saving and economic returns using multicriteria analysis applied to cotton. *Biosyst. Eng.* **2014**, *122*, 74–90. [CrossRef]
- Darouich, H.; Cameira, R.M.; Gonçalves, J.M.; Paredes, P.; Pereira, L.S. Comparing sprinkler and surface irrigation for wheat using multi-criteria analysis: Water saving vs. economic returns. *Water* **2017**, *9*, 50. [CrossRef]
- Janat, M. Efficiency of nitrogen fertilizer for potato under fertigation utilizing a nitrogen tracer technique. *Commun. Soil Sci. Plant Anal.* **2007**, *38*, 2401–2422. [CrossRef]
- Halwani, J.; Baroudi, B.O.; Wartel, M. Nitrate contamination of the groundwater of the Akkar Plain in northern Lebanon. *Sante* **1999**, *9*, 219–223.
- Abou Zakhem, B.; Hafez, R. Environmental isotope study of seawater intrusion in the coastal aquifer (Syria). *Environ. Geol.* **2007**, *51*, 1329–1339. [CrossRef]
- Kattaa, B.; Al-Fares, W.; Al Charideh, A.R. Groundwater vulnerability assessment for the Banyas Catchment of the Syrian coastal area using GIS and the RISKE method. *J. Environ. Manag.* **2010**, *91*, 1103–1110. [CrossRef]
- Chard, E.D. An Economic Analysis of the Akkar Plain Project. Ph.D. Thesis, Utah State University, Logan, UT, USA, 1981. Paper 4210.
- Castel, J.R. Water use of developing citrus canopies in Valencia, Spain. In Proceedings of the IX Congress of the International Society of Citriculture, Orlando, FL, USA, 3–7 December 2000.
- Snyder, R.L.; O’Connell, N.V. Crop coefficients for microsprinkler-irrigated, clean-cultivated, mature citrus in an arid climate. *J. Irrig. Drain. Eng.* **2007**, *33*, 43–52. [CrossRef]
- Villalobos, F.J.; Testi, L.; Orgaz, F.; García-Tejera, O.; Lopez-Bernal, A.; González-Dugo, M.V.; Ballester-Lurbe, C.; Castel, J.R.; Alarcón-Cabañero, J.J.; Nicolás-Nicolás, E.; et al. Modelling canopy conductance and transpiration of fruit trees in Mediterranean areas: A simplified approach. *Agric. Forest Meteorol.* **2013**, *171–172*, 93–103. [CrossRef]
- Consoli, S.; Vanella, D. Mapping crop evapotranspiration by integrating vegetation indices into a soil water balance model. *Agric. Water Manag.* **2014**, *143*, 71–81. [CrossRef]
- Taylor, N.J.; Annandale, J.G.; Vahrmeijer, J.T.; Ibraimo, N.A.; Mahohoma, W.; Gush, M.B.; Allen, R.G. Modelling water use of subtropical fruit crops: The challenges. *Acta Hort.* **2017**, *1160*, 277–284. [CrossRef]
- Peddinti, S.R.; Kambhammettu, B.V.N.P. Dynamics of crop coefficients for citrus orchards of central India using water balance and eddy covariance flux partition techniques. *Agric. Water Manag.* **2019**, *212*, 68–77. [CrossRef]

28. Rallo, G.; González-Altozano, P.; Manzano-Juárez, J.; Provenzano, G. Using field measurements and FAO-56 model to assess the eco-physiological response of citrus orchards under regulated deficit irrigation. *Agric. Water Manag.* **2017**, *180*, 136–147. [[CrossRef](#)]
29. Jafari, M.; Kamali, H.; Keshavarz, A.; Momeni, A. Estimation of evapotranspiration and crop coefficient of drip-irrigated orange trees under a semi-arid climate. *Agric. Water Manag.* **2021**, *248*, 106769. [[CrossRef](#)]
30. García-Tejero, I.; Durán-Zuazo, V.H.; Arriaga-Sevilla, J.; Muriel Fernández, J.L. Impact of water stress on citrus yield. *Agron. Sustain. Dev.* **2012**, *32*, 651–659. [[CrossRef](#)]
31. Er-Raki, S.; Chehbouni, A.; Guemouria, N.; Ezzahar, J.; Khabba, S.; Boulet, G.; Hanich, L. Citrus orchard evapotranspiration: Comparison between eddy covariance measurements and the FAO-56 approach estimates. *Plant Biosyst.* **2009**, *143*, 201–208. [[CrossRef](#)]
32. Martínez-Gimeno, M.A.; Bonet, L.; Provenzano, G.; Badal, E.; Intrigliolo, D.S.; Ballester, C. Assessment of yield and water productivity of clementine trees under surface and subsurface drip irrigation. *Agric. Water Manag.* **2018**, *206*, 209–216. [[CrossRef](#)]
33. García Tejero, I.; Durán Zuazo, V.H.; Jiménez Bocanegra, J.A.; Muriel Fernández, J.L. Improved water-use efficiency by deficit-irrigation programmes: Implications for saving water in citrus orchards. *Sci. Hort.* **2011**, *128*, 274–282. [[CrossRef](#)]
34. Ballester, C.; Castel, J.; Intrigliolo, D.S.; Castel, J.R. Response of Clementina de Nules citrus trees to summer deficit irrigation. Yield components and fruit composition. *Agric. Water Manag.* **2011**, *98*, 1027–1032. [[CrossRef](#)]
35. Allen, R.G.; Pereira, L.S.; Howell, T.A.; Jensen, M.E. Evapotranspiration information reporting: I. Factors governing measurement accuracy. *Agric. Water Manag.* **2011**, *98*, 899–920. [[CrossRef](#)]
36. Allen, R.G.; Pereira, L.S.; Howell, T.A.; Jensen, M.E. Evapotranspiration information reporting: II. Recommended documentation. *Agric. Water Manag.* **2011**, *98*, 921–929. [[CrossRef](#)]
37. Allen, R.G.; Pereira, L.S.; Raes, D.; Smith, M. *Crop Evapotranspiration—Guidelines for Computing Crop Water Requirements*; Irrigation & Drainage Paper 56; Food and Agriculture Organization of the United Nations (FAO): Rome, Italy, 1998.
38. Rallo, G.; Paço, T.A.; Paredes, P.; Puig-Sirera, À.; Massai, R.; Provenzano, G.; Pereira, L.S. Updated single and dual crop coefficients for tree and vine fruit crops. *Agric. Water Manag.* **2021**, *250*, 106645. [[CrossRef](#)]
39. Pereira, L.S.; Allen, R.G.; Smith, M.; Raes, D. Crop evapotranspiration estimation with FAO56: Past and future. *Agric. Water Manag.* **2015**, *147*, 4–20. [[CrossRef](#)]
40. Pereira, L.S.; Paredes, P.; Jovanovic, N. Soil water balance models for determining crop water and irrigation requirements and irrigation scheduling focusing on the FAO56 method and the dual Kc approach. *Agric. Water Manag.* **2020**, *241*, 106357. [[CrossRef](#)]
41. López-Urrea, R.; Martín de Santa Olalla, F.; Montoro, A.; López-Fuster, P. Single and dual crop coefficients and water requirements for onion (*Allium cepa* L.) under semiarid conditions. *Agric. Water Manag.* **2009**, *96*, 1031–1036. [[CrossRef](#)]
42. Paço, T.; Ferreira, M.; Rosa, R.; Paredes, P.; Rodrigues, G.; Conceição, N.; Pacheco, C.; Pereira, L. The dual crop coefficient approach using a density factor to simulate the evapotranspiration of a peach orchard: SIMDualKc model versus eddy covariance measurements. *Irrig. Sci.* **2012**, *30*, 115–126. [[CrossRef](#)]
43. Kool, D.; Agam, N.; Lazarovitch, N.; Heitman, J.L.; Sauer, T.J.; Ben-Gal, A. A review of approaches for evapotranspiration partitioning. *Agric. For. Meteorol.* **2014**, *184*, 56–70. [[CrossRef](#)]
44. González, M.G.; Ramos, T.B.; Carlesso, R.; Paredes, P.; Petry, M.T.; Martins, J.D.; Aires, N.P.; Pereira, L.S. Modelling soil water dynamics of full and deficit drip irrigated maize cultivated under a rain shelter. *Biosyst. Eng.* **2015**, *132*, 1–18. [[CrossRef](#)]
45. Rosa, R.D.; Paredes, P.; Rodrigues, G.C.; Alves, I.; Fernando, R.M.; Pereira, L.S.; Allen, R.G. Implementing the dual crop coefficient approach in interactive software. 1. Background and computational strategy. *Agric. Water Manag.* **2012**, *103*, 8–24. [[CrossRef](#)]
46. Martins, J.D.; Rodrigues, G.C.; Paredes, P.; Carlesso, R.; Oliveira, Z.B.; Knies, A.E.; Petry, M.T.; Pereira, L.S. Dual crop coefficients for maize in southern Brazil: Model testing for sprinkler and drip irrigation and mulched soil. *Biosyst. Eng.* **2013**, *115*, 291–310. [[CrossRef](#)]
47. Zhao, N.N.; Liu, Y.; Cai, J.B.; Rosa, R.; Paredes, P.; Pereira, L.S. Dual crop coefficient modelling applied to the winter wheat-summer maize crop sequence in North China Plain: Basal crop coefficients and soil evaporation component. *Agric. Water Manag.* **2013**, *117*, 93–105. [[CrossRef](#)]
48. Paredes, P.; Rodrigues, G.C.; Alves, I.; Pereira, L.S. Partitioning evapotranspiration, yield prediction and economic returns of maize under various irrigation management strategies. *Agric. Water Manag.* **2014**, *135*, 27–39. [[CrossRef](#)]
49. Paredes, P.; D’Agostino, D.; Assif, M.; Todorovic, M.; Pereira, L.S. Assessing potato transpiration, yield and water productivity under various water regimes and planting dates using the FAO dual Kc approach. *Agric. Water Manag.* **2018**, *195*, 11–24. [[CrossRef](#)]
50. Zhang, H.; Huang, G.; Xu, X.; Xiong, Y.; Huang, Q. Estimating evapotranspiration of processing tomato under plastic mulch using the SIMDualKc model. *Water* **2018**, *10*, 1088. [[CrossRef](#)]
51. Rosa, R.D.; Paredes, P.; Rodrigues, G.C.; Fernando, R.M.; Alves, I.; Pereira, L.S.; Allen, R.G. Implementing the dual crop coefficient approach in interactive software: 2. Model testing. *Agric. Water Manag.* **2012**, *103*, 62–77. [[CrossRef](#)]
52. Darouich, H.; Karfoul, R.; Eid, H.; Ramos, T.B.; Baddour, N.; Moustafa, A.; Assaad, M.I. Modeling zucchini squash irrigation requirements in the Syrian Akkar region using the FAO56 dual-Kc approach. *Agric. Water Manag.* **2020**, *229*, 105927. [[CrossRef](#)]
53. Darouich, H.; Karfoul, R.; Ramos, T.B.; Moustafa, A.; Shaheen, B.; Pereira, L.S. Crop water requirements and crop coefficients for jute mallow (*Corchorus olitorius* L.) using the SIMDualKc model and assessing irrigation strategies for the Syrian Akkar region. *Agric. Water Manag.* **2021**, *255*, 107038. [[CrossRef](#)]

54. Köppen, W. Die Wärmezonen der Erde, nach der Dauer der heissen, gemässigten und kalten Zeit und nach der Wirkung der Wärme auf die organische Welt betrachtet. *Meteorol. Z.* **1884**, *1*, 215–226.
55. FAO; IIASA; ISRIC; ISS-CAS; JRC. *Harmonized World Soil Database (Version 1.1)*; FAO: Rome, Italy; IIASA: Laxenburg, Austria, 2009.
56. IUSS Working Group. *World Reference Base for Soil Resources 2014: International Soil Classification System for Naming Soils and Creating Legends for Soil Maps*; World Soil Resources Reports No. 106; Food and Agriculture Organization of the United Nations (FAO): Rome, Italy, 2014.
57. Coops, N.; Loughhead, A.; Ryan, P.; Hutton, R. Development of daily spatial heat unit mapping from monthly climatic surfaces for the Australian continent. *Int. J. Geogr. Inf. Syst.* **2001**, *15*, 345–361. [[CrossRef](#)]
58. Luo, Q. Temperature thresholds and crop production: A review. *Clim. Chang.* **2011**, *109*, 583–598. [[CrossRef](#)]
59. Samaradiwakara, S.D.; Champa, W.A.H.; Eeswara, J.P. Effect of thermal summation on harvest maturity of Citrus aurantifolia Swingle ‘Local’. *Acta hortic.* **2020**, *1278*, 53–58. [[CrossRef](#)]
60. González-Altozano, P.; Castel, J.R. Regulated deficit irrigation in ‘Clementina de Nules’ citrus trees. II: Vegetative growth. *J. Hortic. Sci. Biotechnol.* **2000**, *75*, 388–392. [[CrossRef](#)]
61. García-Tejero, I.; Romero-Vicente, R.; Jiménez-Bocanegra, J.A.; Martínez-García, G.; Durán-Zuazo, V.H.; Muriel-Fernández, J.L. Response of citrus trees to deficit irrigation during different phenological periods in relation to yield, fruit quality, and water productivity. *Agric. Water Manag.* **2010**, *97*, 689–699. [[CrossRef](#)]
62. Merriam, J.L.; Keller, I. *Farm Irrigation System Evaluation: A Guide for Management*; Utah State University: Logan, UT, USA, 1978.
63. Pereira, L.S.; Paredes, P.; Hunsaker, D.J.; López-Urrea, R.; Jovanovic, N. Updates and advances to the FAO56 crop water requirements and methods. *Agric. Water Manag.* **2021**, *248*, 106697. [[CrossRef](#)]
64. Liu, Y.; Pereira, L.S.; Fernando, R.M. Fluxes through the bottom boundary of the root zone in silty soils: Parametric approaches to estimate groundwater contribution and percolation. *Agric. Water Manag.* **2006**, *84*, 27–40. [[CrossRef](#)]
65. Allen, R.G.; Wright, J.L.; Pruitt, W.O.; Pereira, L.S.; Jensen, M.E. Water requirements. In *Design and Operation of Farm Irrigation Systems*, 2nd ed.; Hoffman, G.J., Evans, R.G., Jensen, M.E., Martin, D.L., Elliot, R.L., Eds.; ASABE: St. Joseph, MI, USA, 2007; pp. 208–288.
66. Paço, T.A.; Paredes, P.; Pereira, L.S.; Silvestre, J.; Santos, F.L. Crop coefficients and transpiration of a super intensive Arbequina olive orchard using the dual Kc approach and the Kcb computation with the fraction of ground cover and height. *Water* **2019**, *11*, 383. [[CrossRef](#)]
67. Darouich, H.; Ramos, T.B.; Pereira, L.S.; Rabino, D.; Bagagiolo, G.; Capello, G.; Simionesei, L.; Cavallo, E.; Biddoccu, M. Water use and soil water balance of Mediterranean vineyards under rainfed and drip irrigation management. Evapotranspiration partition, soil management and resource conservation. *Water* **2022**, *14*, 554. [[CrossRef](#)]
68. Allen, R.G.; Pereira, L.S.; Smith, M.; Raes, D.; Wright, J.L. FAO-56 dual crop coefficient method for estimating evaporation from soil and application extensions. *J. Irrig. Drain. Eng.* **2005**, *131*, 2–13. [[CrossRef](#)]
69. Allen, R.G.; Pereira, L.S. Estimating crop coefficients from fraction of ground cover and height. *Irrig. Sci.* **2009**, *28*, 17–34. [[CrossRef](#)]
70. Pereira, L.S.; Paredes, P.; Melton, F.; Johnson, L.; Wang, T.; López-Urrea, R.; Cancela, J.J.; Allen, R. Prediction of crop coefficients from fraction of ground cover and height. Background and validation using ground and remote sensing data. *Agric. Water Manag.* **2020**, *240*, 106197. [[CrossRef](#)]
71. Pereira, L.S.; Paredes, P.; Melton, F.; Johnson, L.; Mota, M.; Wang, T. Prediction of crop coefficients from fraction of ground cover and height: Practical application to vegetable, field, and fruit crops with focus on parameterization. *Agric. Water Manag.* **2021**, *252*, 106663. [[CrossRef](#)]
72. Pereira, L.S.; Paredes, P.; Rodrigues, G.C.; Neves, M. Modeling malt barley water use and evapotranspiration partitioning in two contrasting rainfall years. Assessing AquaCrop and SIMDualKc models. *Agric. Water Manag.* **2015**, *159*, 239–254. [[CrossRef](#)]
73. Nash, J.E.; Sutcliffe, J.V. River flow forecasting through conceptual models part I—A discussion of principles. *J. Hydrol.* **1970**, *10*, 282–290. [[CrossRef](#)]
74. Legates, D.; McCabe, G. Evaluating the use of goodness of fit measures in hydrologic and hydroclimatic model validation. *Water Resour. Res.* **1999**, *35*, 233–241. [[CrossRef](#)]
75. Moriasi, D.N.; Arnold, J.G.; Van Liew, M.W.; Bingner, R.L.; Harmel, R.D.; Veith, T.L. Model evaluation guidelines for systematic quantification of accuracy in watershed simulations. *Trans. ASABE* **2007**, *50*, 885–900. [[CrossRef](#)]
76. Fandiño, M.; Cancela, J.J.; Rey, B.J.; Martínez, E.M.; Rosa, R.G.; Pereira, L. Using the dual-Kc approach to model evapotranspiration of Albariño vineyards (*Vitis vinifera* L. cv. Albariño) with consideration of active ground cover. *Agric. Water Manag.* **2012**, *112*, 75–87. [[CrossRef](#)]
77. Cancela, J.J.; Fandiño, M.; Rey, B.J.; Martínez, E.M. Automatic irrigation system based on dual crop coefficient, soil and plant water status for *Vitis vinifera* (cv Godello and cv Mencía). *Agric. Water Manag.* **2015**, *151*, 52–63. [[CrossRef](#)]
78. Silva, S.P.; Valín, M.I.; Mendes, S.; Araujo-Paredes, C.; Cancela, J.J. Dual crop coefficient approach in *Vitis vinifera* L. cv. Loureiro. *Agronomy* **2021**, *11*, 2062. [[CrossRef](#)]

79. Paço, T.A.; Pôças, I.; Cunha, M.; Silvestre, J.C.; Santos, F.L.; Paredes, P.; Pereira, L.S. Evapotranspiration and crop coefficients for a super intensive olive orchard. An application of SIMDualKc and METRIC models using ground and satellite observations. *J. Hydrol.* **2014**, *519*, 2067–2080. [[CrossRef](#)]
80. Puig-Sirera, À.; Rallo, G.; Paredes, P.; Paço, T.A.; Minacapilli, M.; Provenzano, G.; Pereira, L.S. Transpiration and water use of an irrigated traditional olive grove with sap-flow observations and the FAO56 dual crop coefficient approach. *Water* **2021**, *13*, 2466. [[CrossRef](#)]